Christian Cziezerski

Development of an RF Device Test Solution for RFID Base Stations

Helsinki Metropolia University of Applied Sciences

Bachelor of Engineering

Electronics

Thesis

May 2014

Helsinki Metropolia University of Applied Sciences

Author Title Number of Pages Date	Christian Cziezerski Development of Test Methods for RFID Base Stations 41 pages + 16 appendices 15 May 2014
Degree	Bachelor of Engineering
Degree Programme	Electronics
Instructor/ Supervisor	Thierry Baills, Senior Lecturer Jarmo Kivinen, Head of Radio Electronics Development at MariSense Oy

The objective of the thesis was to develop a test fixture solution for the device verification process (functional test/documentation) of an RFID base station against regulatory specifications of the FCC and ETSI authorities. Differences between EIRP/ERP and electric field strength needed to be explained.

The project was carried out with actual production devices in the premises of the production site of MariSense Oy, as independent work in the R&D RF-laboratory and anechoic chamber.

A microwave test fixture was designed with an optional interface for future integration in Automatic Test Equipment. The performance characteristics of the fixture were determined and documented. The required normative references were identified and are summarised in a specification table.

The test fixture solution proves to be very useful in the device verification process, and provides a good base for an automatized test system. Additional calibration considerations and performance changes due to temperature variations should be examined.

Keywords	RFID Base Station, RF testing, 915 MHz, 868 MHz

Table of Contents

List of Figures

List of Tables

List of Equations

Abbreviations

$\theta_{3\ dB}$	Antenna Beamwitdh
ACI	Adjacent Channel Interference
ACS	Adjacent Channel Selectivity
ACSR	Adjacent Channel Selectivity Ratio
AIDC	Automatic Identification and Data Capture
API	Application programming interface
ATE	Automatic Test Equipment
BW	Bandwidth
CCI	Co-Channel Interference
CCRR	Co-Channel Rejection Ratio
CFR	Code of Federal Regulations
DUT	Device under test
EBS	Ella® Base Station
ECC	Electronic Communications Committee
EIRP	Equivalent Isotropic Radiated Power in decibel
eirp	Equivalent Isotropic Radiated Power in Watt
EN	European Standard by the European Committee for Standardization
ERP	Effective Radiated Power in decibel
erp	Effective Radiated Power in Watt
ETSI	European Telecommunications Standards Institute
FCC	Federal Communications Commission
GPIB	General Purpose Interface Bus, i.e. IEEE-488
GUI	Graphical User Interface
IEEE	Institute of Electrical and Electronics Engineers
ISM-band	Industrial, scientific and medical radio band
ITU	International Telecommunication Union
LXI	LAN eXtensions for Instrumentation
OATS	Open Air Test Site
OCR	Optical Character Recognition
PAD	RF Power Attenuator Device
PoE	Power over Ethernet

PXI	PCI eXtensions for Instrumentation
RBW	Resolution bandwidth
RF	Radio Frequency
RFID	Radio Frequency Identification Device
SA	Spectrum Analyser
SCPI	Standard Commands for Programmable Instruments
SNR	Signal to Nose Ratio
SRD	Short Range Device
VISA	Virtual Instrument Software Architecture
VNA	Vector Network Analyser
VSWR	Voltage Standing Wave Ratio

1 Introduction

MariSense Oy's main product line, the Ella® wireless shelf label (ESL), is a novel combination of the brilliant paper-like experience of e-ink with the convenience of an RFID controlled electronic price display. The Ella® retail system operates as unlicensed device in the 868 MHz ISM band, and can be classified as an RFID-system that consists of an Ella® base station, EBS (the reader), and the shelf label (the transponder).

MariSense Oyis a small Finnish company based out of Tuusula, which specialises in complete retail store label and store control solutions. In order to expand its business to the FCC region, MariSense Oy needed the RF-testing procedure of the EBS modified and adapted to comply with the regulatory standards for wireless communication for the 902...928 MHz ISM band. The specifications for this frequency band had to be researched; they are governed by the FCC in Title 47 Code of Federal Regulations Part 15 and Part 18.

Test fixtures typically form the centre point for the RF-tests involved in transmitter and receiver tests of RF-devices. For MariSense Oy in particular, the purpose of this study is to satisfy the need for such a test fixture solution, and also to develop test methods for the fixture as it is used in the transceiver verification process of the Ella® Base Station.

1.1 Organisation of the Thesis

Part one introduces the subject of the thesis and the company that provided the thesis topic. The goal of the project is briefly mentioned.

Part two provides an overview of the subject area and the background of the project. The goal is set within the scope of the project.

Part three describes the methods used in RF device testing. It introduces the normative bodies that govern the regulations which form the basis for RF-test specifications, and clarifies how and why these are relevant to the test fixture developed for MariSense Oy.

Part four presents the realisation of the test fixture that was developed for the project and its capabilities related to the goal.

Part five discusses and reviews the implementation of the project, and finally

Part 6 summarises the project and presents the conclusion.

2 Background

RFID is generally a non-contact transmission of data via RF waves and typically consists of at least one transponder with some kind of memory, and a reader device. RFID technology is part of the auto-ID technology AIDC, like for example barcodes or the optical character recognition OCR.

2.1 Regulatory Bodies, License Free Frequency Band

Because radio waves are used to transmit the data, RFID systems are typically operated in an ISM frequency band so that the end-user of the system is not required to obtain a license for operating an RF device [1] [2]. This however, does not mean that the devices are free from other regulatory restrictions. In fact, there are very detailed rules and regulations that cover the allocation and use of the radio spectrum so that technology may interconnect seamlessly.

The global allocation of the radio spectrum is managed by the International Telecommunication Union. The ITU further publishes standards, or recommendations, that are fundamental to the operation of the communication networks. The ITU divides the world into three so-called ITU regions, as seen in Figure 1, for purposes of frequency allocation. [3]

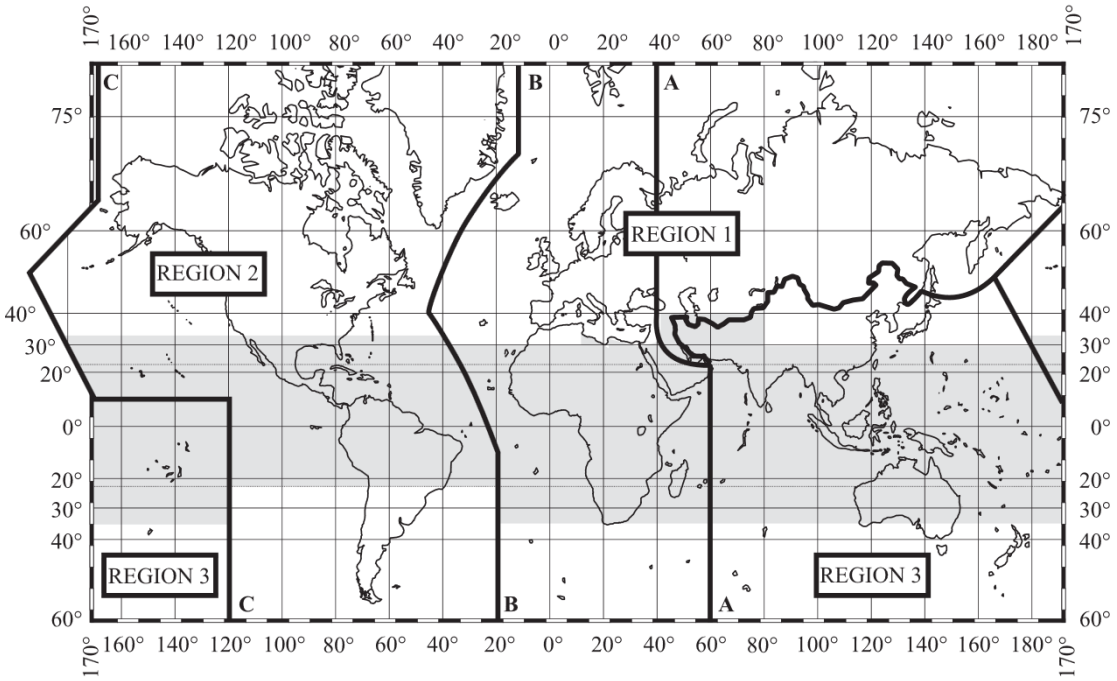

Figure 1. ITU Frequency Regions as per ITU RR5-2. [3, p. 37]

Figure 1 depicts the world as it is divided into three major regions. Region 1 includes all territory bounded to the west by the line marked as B and bounded to the east by line A. Additionally, all of the northern part of the Russian Federation bounded by the Lines A and C belongs to Region 1.

Region 2 is all of the territory bounded by the lines C and B.

Region 3 is the territory bounded by the lines A to the west, C to the east and the line in the north that follows the border of, amongst others, Turkey, Ukraine and the Russian Federation.

In the United States, which lies in region 2, the key regulatory body for (not only) radio communication is the government agency FCC. The corresponding organisation responsible for communication technologies in Europe, which lies in region 1, is the ETSI [4]. The regulations issued by these entities provide the background for the specifications and test methods used for the RF device test solution developed in this thesis.

Frequency bands of interest within the scope of this thesis and their permissible power are summarised in Table 1:

Table 1. License Free Frequency Bands used by EllaRetail®

Region	Frequency	Radiated power
1 – Europe	865.6-867.6 MHz	2 W erp [1] [5]
2 – Americas	902-928 MHz	+36 dBm EIRP [6]

As can be seen from the radiated power column in Table 1, there are different methods of describing radiated power. The differences between the specifications of radiated power, and conversion between them, will be explained in part three.

2.2 Objective, Scope and Limitations

The device testing at MariSense Oy was conducted manually, with varying setup parameters like for example different cables of changing quality, the door of the anechoic chamber open or partially closed. Testing was generally slow and results could vary enough

to potentially violate specifications. With the addition of ITU Region 2 (Americas) customers, additional tests would be required once the additional test specifications are defined and the references identified.

This thesis aims at developing a permanent test fixture together with test methods for the RF-transceiver, in particular tests for conducted transmitter output power and harmonics, in order to improve repeatability, reproducibility and to help overcome some of the issues that arise with test setup variations and limited mating cycles of cheap cable connectors.

The test-fixture solution was required to provide a low-cost rudimental ATE interface with the ability to interface with legacy GPIB equipment available in MariSense Oy's RF laboratory. Modern communication test equipment such as a PXI/LXI test rack with real-time signal synthesis was out of question due to budget constraints. The general lack of resources and the restricted amount of time available limited the otherwise very comprehensive project. As a consequence, calibration and drift due to temperature changes were ignored and only a few important transceiver tests were implemented. Additionally, EMC and other unwanted conducted and radiated emission tests were not handled in this thesis. Measurement uncertainties are not handled here and will be understood as known and calculated in accordance with ETSI. [7]

3 Methods and Materials

This part describes the differences between the tree specifications of radiated power and how to easily convert from one to the other. It then explains the typical methods required in RF device testing. It further introduces the normative bodies that govern the relevant regulations, and briefly explains to what extent these are relevant to the test fixture developed for MariSense Oy.

3.1 Power in EIRP, ERP and E-Field

As already mentioned in the previous part, there are different ways in which the normative references describe the enrgy of radiated power [4, p. 2]:

- The effective isotropic radiated power in Watt eirp or dBm EIRP,
- The effective radiated power in Watt erp or dBm ERP, and
- The electric field strength E, measured at some distance *r* from the radiator.

EIRP is the effective radiated isotropic power, i.e. the power that would have to be supplied to a perfectly isotropic radiator in order to achieve the same electric field strength that the DUT produces at the same distance.

ERP is similar to EIRP with the exception of it being the electric field relative to a half-wave dipole instead of an isotropic antenna. In other words, it is the power supplied to an antenna multiplied by the gain of the antenna referenced to a dipole (dBd). The reason for referencing to a dipole is, that the half-wave dipole is a better representation of a realistic antenna.

The relationship between EIRP and ERP comes from the maximum theoretical antenna gain of the dipole $G_{dipole} = 1.64$ [8, p. 52], which is expressed relative to an isotropic antenna in terms of dBi:

Gain of a dipole:

$$\log G_{dipole} = 10 \cdot \log 1.64 = 2.15\ dBi \tag{3-1}$$

Since the gain of a perfect isotropically radiating antenna referenced to itself is $G_{isotropic} = 1 \ (\equiv 0 \ dBi)$, the conversion between EIRP and ERP can be determined by the following relationships [9, p. 13] :

From ERP to EIRP

$$EIRP = ERP + 2.15 \ dB \tag{3-2}$$

From EIRP to ERP

$$ERP = EIRP - 2.15 \ dBi \tag{3-3}$$

Especially in normative references from the FCC, radiated emissions are specified in electrical field strength at a distance of 3m, rather than power in EIRP or ERP. In order to be able to conveniently compare between the different normative references, it is thus necessary to find an equation that describes this relationship.

As already mentioned before, EIRP is the power that would have to be supplied to an isotropic radiator in order to get the same electric field strength that the DUT produces at this distance. Therefore, if the electric field strength is known, the EIRP can be found via the following equation:

From Electric Field Strength to EIRP[1] [4, p. 2]:

$$\begin{aligned} EIRP &= 10 \cdot \log\left(\frac{4\pi \cdot E^2 \cdot r^2}{0.377 \ [V^2]}\right) dBm \\ &= 10 \cdot \log\left(\frac{E^2 \cdot r^2}{0.030 \ [V^2]}\right) \ dBm \end{aligned} \tag{3-4}$$

[1] For a complete derivation of the formula, see Appendix A – From Electric Field Strength to EIRP.

Where:

$EIRP$: The Effective Isotropic Power in *dBm*,

E : The electrical field strength in $\frac{V}{m}$

r : The distance from the transmitting antenna in *m*, and

V : is the unit of measurement (*Volt*).

Thus, if any one of the three terms EIRP, ERP or the electric field strength E, at the distance r, is known the other two terms can be calculated.

As an example, the transmit power limits and the harmonic, or spurious, emission limits of the 902-928 MHz ISM band and the limits for the 865.6-867.6 MHz ISM band in the US, respectively Europe, are summarised in Table 2, in terms of electric field strength, EIRP and ERP [2, pp. 247, 249] [10, p. 33] [5, p. 28]:

Table 2. Transmitter Power and Harmonic Limits in E, EIRP and ERP

Frequency [MHz]	Fundamental			Harmonics/Spurious		
	E [V/m][2]	EIRP [dBm]	ERP [dBm]	E [V/m]	EIRP [dBm]	ERP [dBm]
902-928[3]	3.64	+36	+33.85	$364 \cdot 10^{-3}$	+16[4]	+13.85
902-928[5]				$500 \cdot 10^{-6}$	−41.23	−43.38
865.6-867.6[6]	2.58	+35.15	+33[7]	$1.43 \cdot 10^{-3}$	−32.15	−30

The limits for 865.6-867.6 MHz in Table 2 are for any spurious emission outside a range of ±500 kHz of the carrier frequency of the DUT. There are additional limits for conducted and radiated spurious emissions below 1 GHz [5].

[2] The electric field strength at a distance of 3 m
[3] With frequency hopping and ≥ 50 channels
[4] For a peak in band emission of +36 dBm EIRP, otherwise -20 dBc within any 100 kHz BW
[5] Where the harmonics fall within a restricted band as per 47 CFR 15.205
[6] For harmonics/spurious > 1 GHz
[7] Value depends on antenna beamwidth

3.2 Compliance Testing of Wireless Equipment

Unlicensed wireless radio equipment placed on the market is subject to compliance testing and certification processes in one form or another. While for the EU market this happens through self-declaration by the manufacturer who supplies the equipment to the market [11], a vendor or manufacturer in the US must apply for FCC certification after careful testing of the device in an authorised laboratory [2].

The detailed compliance testing and certification process for devices in the 902-928 MHz frequency band to the US market, is covered in Title 47 CFR Part 15 of the FCC, summarised in [4], and will not be handled further in this text, as most of the test methods are of similar nature as those for ETSI (similar frequency, similar power, more harmonics etc. but essentially the same methods except for the used detector [12, p. 4.2.1]).

In the EU, the general transceiver specifications and test methods for devices with power levels up to 2 W in the 865-868 MHz band are defined in the European Standard ETSI EN 302 208-1. The methods described by this standard are essentially what the test fixture is required to provide for. The next few paragraphs will handle the most important transmitter and receiver tests as described in this standard.

3.3 Transmitter Tests

The general test conditions like normal, extreme temperature and rel. humidity shall concur with the conditions specified in the EN standard [5, pp. 15-18].

3.3.1 Frequency Error

The frequency error of a radio transmitter is specified as the difference between its nominal frequency and the actual frequency when measured under extreme test conditions. This is important due to the temperature coefficient of the components used in the transceiver; most prominent is the temperature drift of oscillators.

For this test, the DUT is required to transmit a continuous unmodulated carrier at frequencies specified in [5] with a frequency counter connected to its TX output as shown in Figure 2 below:

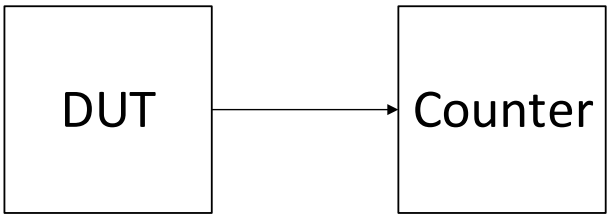

Figure 2. Measurement Setup for Transmitter Frequency Error

A maximum drift of +/-10 ppm is permitted and the frequency error of the test fixture is required to be either at least an order of magnitude better than the frequency error of the DUT or well characterised so that it may be corrected for. For this test it is recommended to use a climate chamber instead of the test fixture due to its large thermal mass.

3.3.2 Frequency Stability under Extreme Voltage Conditions

This test is essentially the same as the frequency error test. However, instead of changing the temperature, the DUT supply voltage will be adjusted to its lower extreme and the frequency of the carrier will be recorded with a frequency counter as illustrated in Figure 3, while the test voltage is further reduced towards zero.

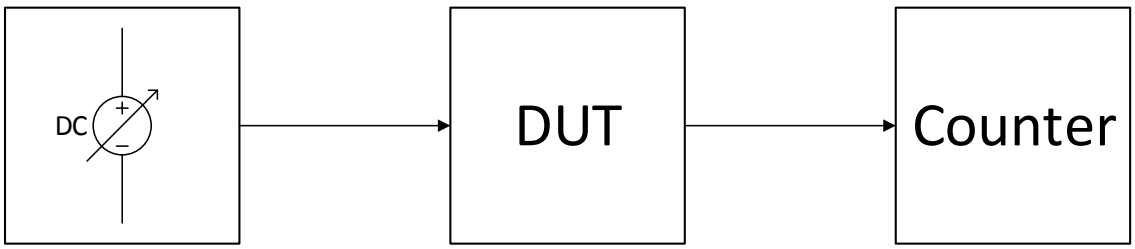

Figure 3. Measurement Setup for Transmitter Frequency Stability

This test is necessary, to verify that the RF-transceiver will still meet its requirements or simply shut down during low states of battery power or brown-out, so that the possible resulting frequency variation does not cause interference. The test fixture meets these requirements by providing external power connectors for system power supplies.

3.3.3 Radiated Power, Conducted Measurement

Perhaps one of the most important tests for a transceiver is the radiated or conducted output power test, since this is the main regulated feature in addition to the frequency.

Many of the tests described in the following sections of this part require that the RF power is measured in some way or another. Although not necessarily mentioned in the measurement methods described in the next sections, cable and path losses will be implied and need to be corrected for as described in this section.

Where the antenna is an integral part of the DUT, tests are typically conducted on a test site such as an Anechoic Chamber or Open Area Test Site (OATS) by mounting the DUT on a turntable at a specific height and at a specified distance away from a test antenna. If the DUT however has external antenna connectors, it is also acceptable to measure the conducted power instead of radiated power. For this, it is sufficient to correct the measured conducted power values for cable loss and antenna gain and state the values in effective radiated power. [5, pp. 22-23]

For production testing, the conducted power measurement method is preferable over the radiated measurement due to the significant cost and complexity of test sites.

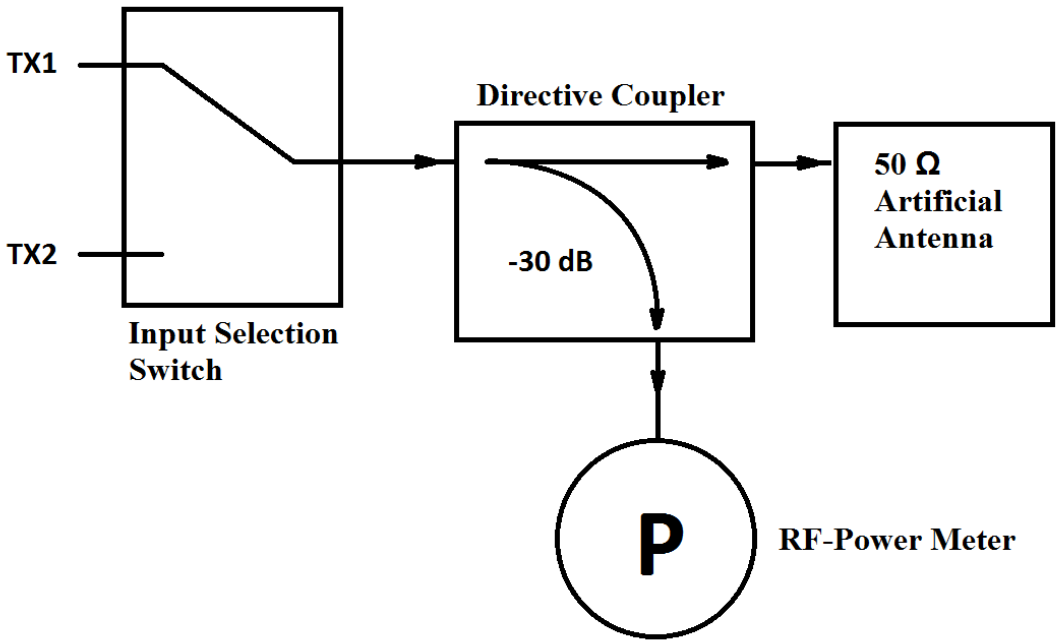

Figure 4. Measurement Setup for Transmitter Power, Conducted Measurement

A method to measure the conducted power is illustrated in Figure 4. RF power is conducted from the TX antenna connectors to an input selection switch. From there, the signal passes through a directive coupler and terminates into a 50 Ω dummy load which

simulates an antenna. Where the DUT has multiple antenna connectors, it is necessary to provide means to switch between them since the measurement has to be repeated for each output. In the case of the EBS, TX power is only transmitted by one of its two TX connectors at any time. If this were not the case, the transmitted RF power of both connectors would have to be combined with a power divider/combiner. The purpose of the coupler is to provide a non-intrusive approach to measure the peak or mean power. Since power meters are very sensitive instruments and the expected output power of the DUT is in the range of 2 W erp, the selected directive coupler was chosen with a coupling of -30 dBm.

The upper limit for the measured conducted output power of the EBS, when using antennas with circular polarisation with a beamwidth of under 90°, can be calculated with the following equation:

Maximum Allowed Conducted Power [5, p. 23]:

$$P_C = P_{erp} - G_{IC} + 5.15 + C_L \; dBm \tag{3-5}$$

Where:

P_C : Maximum allowed conducted power of the DUT in dBm
P_{erp} : Maximum allowed ERP according to ETSI 302 208-1, which is 33 dBm (2W) for antennas with a beamwidth of $\theta_{3\,dB} \leq 90°$ and 30 dBm (1W) for $\theta_{3\,dB} \leq 180°$
G_{IC} : The antenna gain of a circular antenna in dBiC
C_L : Cable loss in dB

The additional 5.15 dB correction is a result of the fact that the gain of the circular polarised antenna is 3 dB greater than a linear polarised antenna, and that a dipole antenna has an additional 2.15 dB gain compared to an isotropic antenna.

Example:
The antenna used by the EBS has circular polarisation and a gain of $G_{IC} = 5\;dBiC$, and cable loss at 868 MHz is estimated to $C_L = 1.8\;dB$. This gives a maximum allowed conducted output power for an antenna with a beamwidth $\theta_{3\,dB} \leq 90°$ of:

$$P_C = 33\;dBm - 5\;dBiC + 5.15 + 1.8\;dB = 34.95\;dBm\;ERP = 3126\;mW\;erp$$

And for an antenna with a beamwidth of $\theta_{3\,dB} \leq 180°$:

$$P_C = 30\ dBm - 5\ dBiC + 5.15 + 1.8\ dB = 31.95\ dBm\ ERP = 1557\ mW\ erp$$

Furthermore, the power meter reading needs to be corrected for an insertion loss fo the input selection switch of for example 0.1 dB, and for the coupling factor of the directional coupler of -30 dB.

The test fixture can conveniently provide the necessary TX path selection by using co-axial RF-switches.

3.3.4 Transmitter Spectrum Mask

The spectrum mask of the transmitter defines the average power contained in a modulated signal, including the side bands of the carrier, at a range of ±500 kHz around the carrier [5, p. 24].

For this measurement, the DUT is connected to a spectrum analyser as seen in Figure 5 and set to transmit a number of short modulated signal pulses for a sub-band at a carrier frequency fc. The output power of the DUT is then measured with the spectrum analyser, which has to be configured as described in EN 302 208-1.

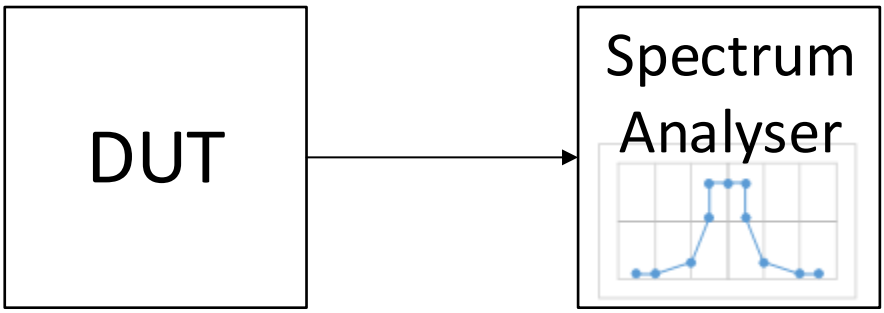

Figure 5. Measurement Setup for Transmitter Spectrum Mask

As implied in Figure 5, the spectrum analyser performs a mask test on the TX signal coming from the DUT.

The point in limiting and measuring the spectrum mask is to make sure that power is not falling into adjacent channels (=Adjacent Channel Power) when the transmitter is switching on and off during normal operation so that interference is limited and also to verify that the occupied bandwidth is used sensibly. The absolute limits of the RF power in ERP for the 868 MHz ISM band spectrum mask are shown in Figure 6 below:

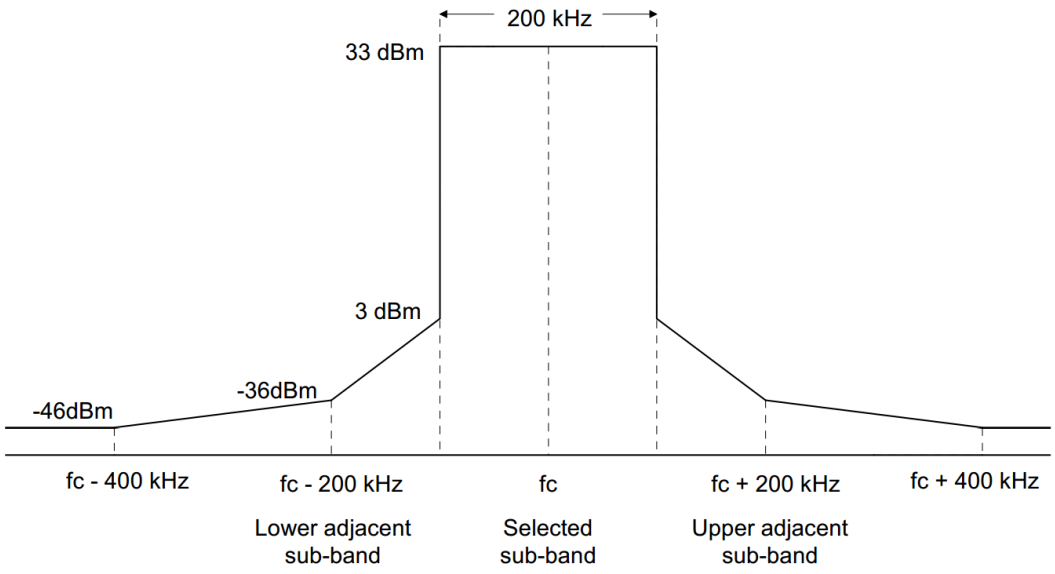

Figure 6. Transmitter Spectrum Mask Limits in ETSI for 865-868 MHz [5]

For the test fixture, the only requirement is to provide means to switch between the two TX connectors and to specify any insertion loss so that the spectrum analyser measurements are compensated for the path loss.

3.3.5 Unwanted Emissions in the Spurious Domain

While the signal spectrum at ±500 kHz around the carrier is specified as the spectrum mask, the unwanted spurious emissions are outside of this frequency range, and contain emissions other than those related to normal modulated transmissions like the carrier and its wanted side bands.

This test aims at detecting and recording the ERP power level of conducted spurious emissions over the frequency range of 30 MHz to 5 GHz with the spectrum analyser configured as described in the standard. Some of the relevant limits for the 868 MHz and the 915 MHz bands were summarised earlier in Table 2. Cabinet radiation is disregarded.

This measurement is conducted in a similar way to the spectrum mask measurement. It too, requires a modulated transmission in short pulses. It can essentially use the same setup with the addition of an attenuator and a selectable high-pass filter, as seen in Figure 7, between the DUT and the spectrum analyser as the spectrum analyser essentially is the measuring receiver that is required for this test. Again, where the DUT has more than one antenna or antenna connector, the measurement has to be repeated for each TX output. [5, p. 26]

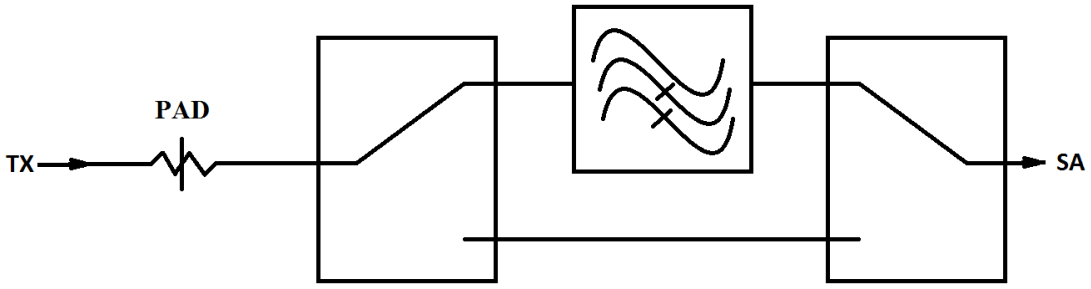

Figure 7. Measurement Setup for Unwanted Spurious Emissions

Ideally, both the spectrum mask test and the spurious emissions test can be executed at the same time, as long as the settings of the spectrum analyser are adjusted as required by the standard. The test fixture must provide means to protect the spectrum analyser from excessive amounts of power. Additionally, the optional high-pass filter in Figure 7 is switched into the signal path on demand, to prevent mixer saturation during measurements above 1 GHz[8]. It also eliminates intermodulation distortion generated in the input of the spectrum analyser. It is in this frequency range that especially the power level of the 2nd to 5th harmonics of the carrier are of interest.

3.3.6 Transmission Time

The transmission time of the DUT is the amount of time that the DUT is continuously transmitting. Not only is the period of time that the DUT is permitted to continuously transmit regulated, but so is the time between two consecutive transmissions and the channel occupancy to ensure that all the channels are used equally. [5, p. 28]

[8] Gain comppression (> 10 MHz) for the HP8590E spectrum analyser is ≤ 0.5 dB (total power at input mixer is equal to -10 dBm) [19, p. 7.10]

This measurement is typically conducted by bringing the DUT in range of a simulated unlimited number of transponders and having an oscilloscope trigger off the transmission antenna of the DUT. The length of the transmission and the interval between two transmissions is recorded.

The test fixture solution already provides means of detecting the transmitted RF-power as described in section 3.3.3. The power meter is thus used to record the transmission length.

3.4 Receiver Tests

The receiver parameters described in EN 302 208-1 are essentially guidelines that are based on compatibility studies conducted by the ECC. A device will not fail compliance tests by violating these recommendations, but it can be assumed that there will be severe degradation in performance of the receiver when exposed to unacceptable levels of interference. [4, pp. 14-15] [5, p. 29]

3.4.1 Co-Channel Rejection

Co-channel interference (CCI) happens when a DUT receives multiple transmissions on the same channel at the same time. Thus, co-channel rejection is a measure for a receiver's ability to receive a modulated signal without being interrupted by the presence another unwanted signal at the same nominal channel frequency. [5, p. 30]

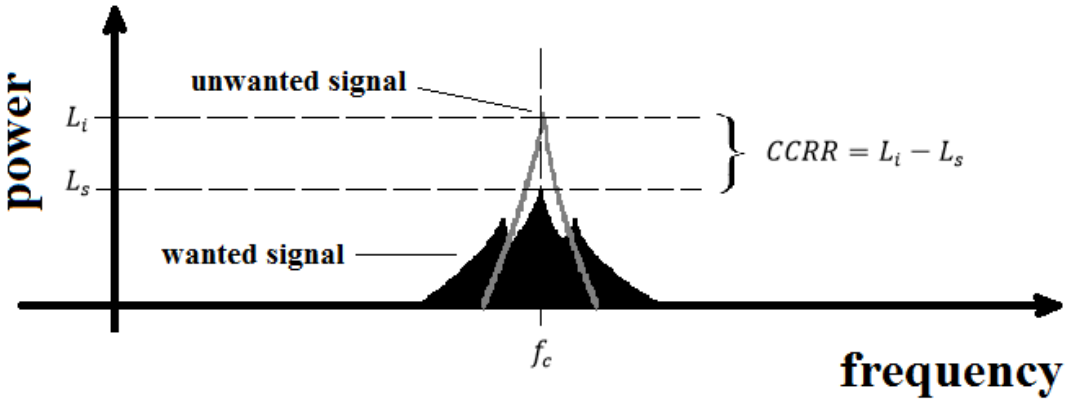

Figure 8. Co-Channel Rejection Ratio

Figure 8 demonstrates one interpretation of the way to quantify co-channel rejection. Here, the co-channel rejection ratio *CCRR* is the ratio of the power L_i of the unwanted, unmodulated interfering signal in grey colour to the power L_s of the modulated wanted signal in black. The CCRR is thus defined as:

Co-Channel Rejection Ratio

$$CCRR = L_i - L_s \tag{3-6}$$

If for example, the level of the wanted signal is set to be 3 dB above the receiver's sensitivity which is known to be -102 dBm, and if the level of the unwanted interfering signal is measured to be -35 dBm, the co-channel rejection ratio can then be determined:

$$CCRR = -35\ dBm - (-102 + 3)\ dBm = 64\ dB$$

This measurement can be performed by using the external antenna connectors of the DUT and a power splitter. It is essentially a crosstalk measurement with two different transmitters which use the same frequency while the receiver attempts to understand only its intended transmission partner.

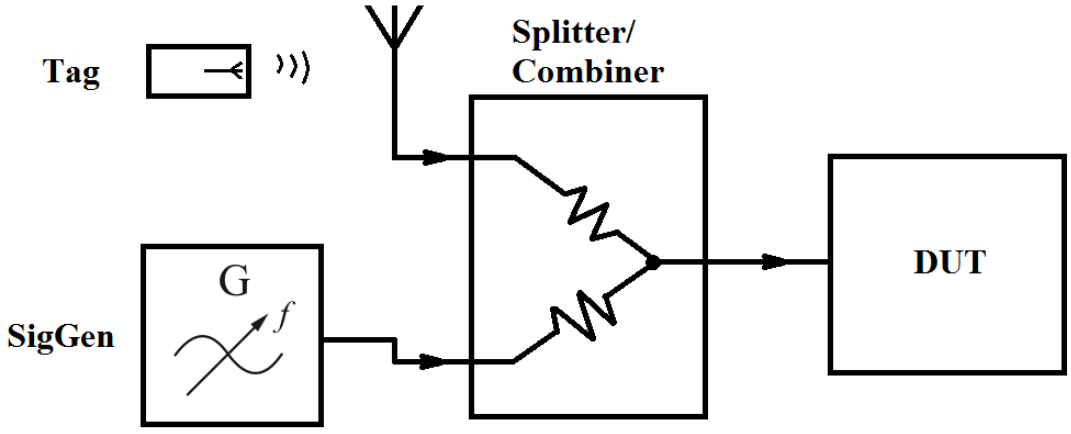

Figure 9. Measurement Setup for Receiver Co-Channel Rejection

As illustrated in Figure 9, a power divider/combiner is used to connect both an antenna and a signal generator to the receiver port of the DUT. The measurement itself involves an active tag that is then placed near the antenna such that the DUT is just barely able to identify it or for example, fails a bit-error specification. This distance r is recorded and

the tag is moved to a distance of $0.7 \cdot r$ away from the antenna, which corresponds to a 3 dB increase in signal power. The signal generator is set to transmit at the same frequency as the tag. The amplitude of the signal generator is then slowly increased until the DUT is unable to identify the tag. Now, the amplitude is again decreased in small steps until the DUT is able to identify the tag again and this signal level is recorded. After compensating the signal levels for combiner-loss and antenna gain, the DUT should be able to reject an unwanted signal of up to -35 dBm ERP. [5, p. 31]

This measurement is of secondary importance for the test fixture, as it is only conducted in the event that the DUT is unable to receive signals at all. The setup can however, be used to investigate receiver sensitivity, i.e. the lowest absolute power at a distance r at which the receiver still can demodulate a received signal.

3.4.2 Adjacent Channel Selectivity

Adjacent channel interference (ACI) happens when a DUT receives a transmission while another unwanted device transmits on an adjacent channel. Thus, adjacent-channel selectivity (ACS) is a measure for a receiver's ability to deal with interferers on frequencies at an offset equal to the channel spacing. The ratio between the wanted and the unwanted signal level is called the adjacent channel selectivity of the receiver. [4, p. 15]

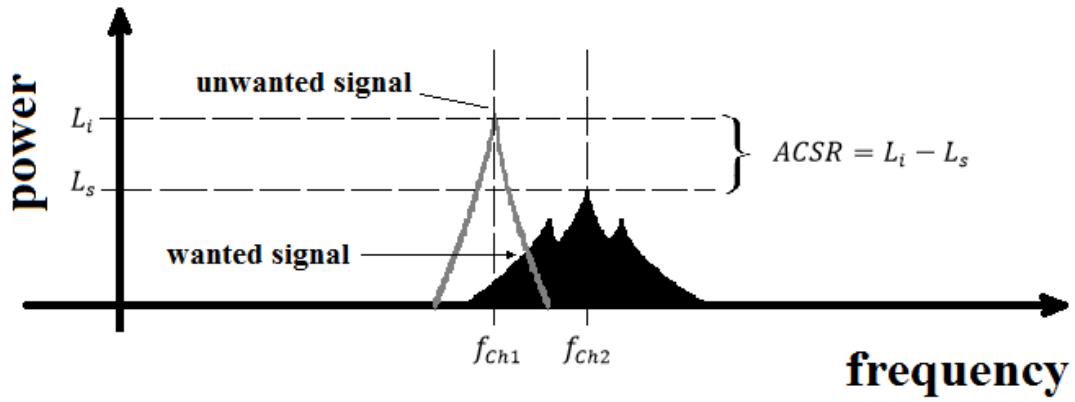

Figure 10. Adjacent Channel Selectivity Ratio

Figure 10 depicts one interpretation of the way to quantify adjacent channel rejection. Here, the adjacent channel selectivity ratio ACS*R* is the ratio of the power L_i of the unwanted, unmodulated interfering signal at a lower adjacent channel Ch1 in grey colour,

to the power L_s of the modulated wanted signal of channel Ch2 in black. The ACSR is thus defined as:
Adjacent Channel Selectivity Ratio

$$ACSR = L_i - L_s \tag{3-7}$$

This measurement is conducted similarly to the test for the co-channel rejection, with reference to Figure 9. The difference is, that the frequency of the signal generator is first set to the upper and then to the lower adjacent channel frequency, meaning the test has to be conducted twice. [5, p. 31]

3.4.3 Blocking or Desensitisation

While the two prior interference or selectivity types were about in-band and adjacent-band interference, the blocking performance of a receiver is evaluated at any frequency other than those frequencies that are covered by the co-channel, adjacent channel and spurious radiation tests. Thus, with reference to the test method in 3.4.1 and Figure 9, the measurement is conducted with the signal generator set at frequencies tuned to an offset of ±1 MHz, ±2 MHz, ±5 MHz and ±10 MHz around the carrier frequency. [5, p. 33]

Phase noise plays a big role for a receiver's blocking capability.

3.4.4 Spurious Emissions

Spurious emissions in receivers can cause a number of uninvited effects ranging from unwanted response over general measurement errors to at the very least, unwanted interference. Internally generated spurs are commonly insignificant but many encountered spurs are actually a product of signals internal to the DUT and external signals. This is the reason why it is so important to identify and possibly eliminate all forms of in-band, adjacent band, out-of-band and spurious emissions.

Spurious emissions from the receiver of the DUT are located outside of the useful bandwidth of the frequency band in which the intentional radiation is taking place. Consequently, the level of the spurious emissions can be reduced without affecting the normal

operation of the receiver. Harmonics, intermodulation distortion, parasitic emissions and frequency conversion products are all spurious emissions. [5, p. 34]
The spurious emissions of receivers are measured in exactly the same way as they are for transmitters, i.e. the conducted power level measured via the antenna connector into an artificial load and via cabinet radiation at a test site as in 3.3.5.

This means that for the test fixture the same measurement setup as illustrated in Figure 7 can be used to connect to a spectrum analyser which will act as wide band receiver from 9 kHz-12.75 GHz. Any spurious components found within this frequency range must be recorded and corrected for attenuator or cable loss in the measurement. The emission limits for the receiver tests are summarised in Table 3:

Table 3. Receiver Emission Limits for the 868 MHz ISM Band in Europe

Test Type	Frequency	Emission Limit	
		erp [W]	ERP [dBm]
Co-Channel Rejection	fc	$\geq 316\,nW$	≥ -35
Adjacent Channel Selectivity	$fc \pm 200\,kHz$	$\geq 316\,nW$	≥ -35
Blocking Performance	$fc \pm 1, \pm 2, \pm 5, \pm 10\,MHz$	$\geq 316\,nW$	≥ -35
Spurious Emissions	$< 1\,GHz$	$2\,nW$	-57
	$> 1\,GHz$	$20\,nW$	-47

3.5 FCC-Required Measurements for RF-Devices

The transmitter and receiver tests methods required for FCC compliance are very similar to those required by the ETSI and will therefore not be explained in detail. Suffice it to say, the test fixture solution developed for this thesis will be able to provide for the majority of required tests without, or with only very minor, modifications.

The required test and limits for the 915 MHz band can be found in Title 47 CFR Part 15 of the FCC. To mention a few important sections that handle transmit power, emission limits and restricted frequency bands of intentional radiators from subpart C of title 47 part 15:

§ 15.205: Restricted bands of operation
§ 15.209: Radiated emission limits
§ 15.247: Operation within the bands 902-928 MHz, […]

§ 15.249: Operation within the bands 902-928 MHz, […]

3.6 Other RF Parameters

There are other parameters that can be used to characterise RF performance of a transceiver some of which require specialised measurement equipment:

- Receiver sensitivity
- Phase noise (special equipment needed)
- Occupied bandwidth (99.5% of total average power lies within this BW)
- Receiver dynamic range (1 dB compression point)

Receiver sensitivity is maybe important enough to be more than only mentioned. It is the weakest possible signal level for which a receiver is still able to meet a particular quality of reception and is therefore closely related to the signal-to-noise ratio, noise figure and the noise floor [13, pp. 24-50]. Sensitivity is defined as:

Sensitivity:

$$S_i = k_B \cdot (T_a + T_{RX}) \cdot BW \cdot \frac{S_0}{N_0} \tag{3-8}$$

Where:

S_i: The Sensitivity in [W]
k_B: Boltzmann's constant
T_a: Equivalent noise temperature of the source in [K]
T_{RX}: Equivalent noise temperature of the receiver referred to the input in [K]
BW: The bandwidth in [Hz]
S_0: Signal power in [W]
N_0: Noise power in [W]

Sensitivity is an important parameter for receivers in general but is not measured for the base stations.

3.7 ATE and Software

Automated Test Equipment is used extensively in manufacturing environments to test if products function as specified. Automated testing is testing that typically runs unattended and evaluates test results without user input. Popular ATE platforms use GPIB, LXI, PXI or legacy serial/parallel ports.

There are several different solutions available to operate an ATE ranging from simple code written in C or C++ over graphical user interfaces in LabVIEW and MATLAB®.

LabVIEW is a graphical programming language which supports a vast range of instrumentation hardware, in particular GPIB and the VISA API, and was therefore chosen to be the base for a future ATE system since all the instruments used in this project are supported by it.

This concludes the methods and materials part. Now follows the results part in which the designed test fixture solution will be presented.

4 Results

This part presents the test fixture that was developed for MariSense Oy and states its specifications in particular the path loss for the transmitter peak out power and harmonics measurements.

4.1 The DUT

The DUT is a circuit board that holds the proprietary transceiver part of MariSense Oy's EBS. It holds a few power connectors, two RX and two TX connectors. It was therefore necessary to provide means to select the ports. The circuit board was mounted onto the fixture and held in place by custom-fit metal pins. As required, high quality durable SMA connectors were used to connect to the RF ports.

4.2 Test Rack Layout

The test fixture as well as supporting measurement equipment and power supplies were arranged in a large 19" test rack with the notion that cabling and instruments should be moved as little as possible. The arrangement can be seen in Figure 11:

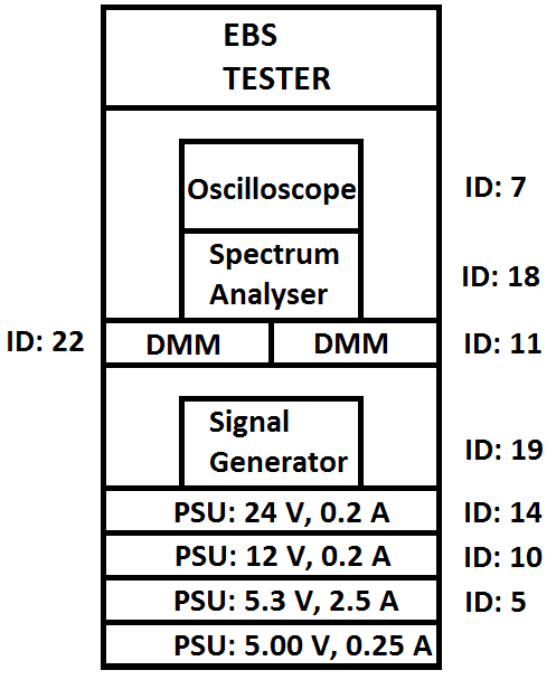

Figure 11. Test Rack Instrument Placement Overview

The actual test fixture is located in the top section followed by an oscilloscope to measure transmission time and gain/phase imbalance of the receiver, a spectrum analyser, a digital multimeter for power rail and power sensor 2 acquisition, a signal generator for receiver tests and various system power supplies to operate and monitor power consumption of the individual transceiver parts. Using a rack was the proper way to implement the device test solution despite its physical dimensions since it provided a permanent test setup.

A photograph of the rack can be seen in appendix [G].

4.3 ATE Interface

All used instruments support GPIB and can be controlled via simple SCPI commands or for example with LabVIEW by using the VISA API. The ID numbers shown in Figure 11 are the GPIB addresses of the instruments.

The coaxial switches and step attenuators of the test fixture can be controlled via a simple remote control box with push-buttons and toggle switches. The remote is connected to the test fixture via an interfacing connector on the front plate. A GPIB switch controller can be connected in place of the remote, thereby providing the required rudimental ATE interface.

A photograph of the front plate of the remote can be found in appendix [G].

4.4 Test Fixture Platform

The test fixture consists of a 50 mm rectangular aluminium profile frame which is a little less than 19” wide, approximately 6 rack units high and about 600 mm deep so that it may fit into a typical 19” Rack. A thick aluminium plate is mounted across the first half of the frame to provide a solid base for the RF-transceiver circuit board and the RF-components that make up the majority of the signal path routing.

The circuit board was fixed with special mounting pins so that it was secured during testing. The front panel consists of 2.5 mm thick aluminium sheet and accommodates a

number of panel mounted SMA connectors, a couple of 4 mm binding posts and a connector for an optional remote control for manual operation of the tester or the ATE interface.

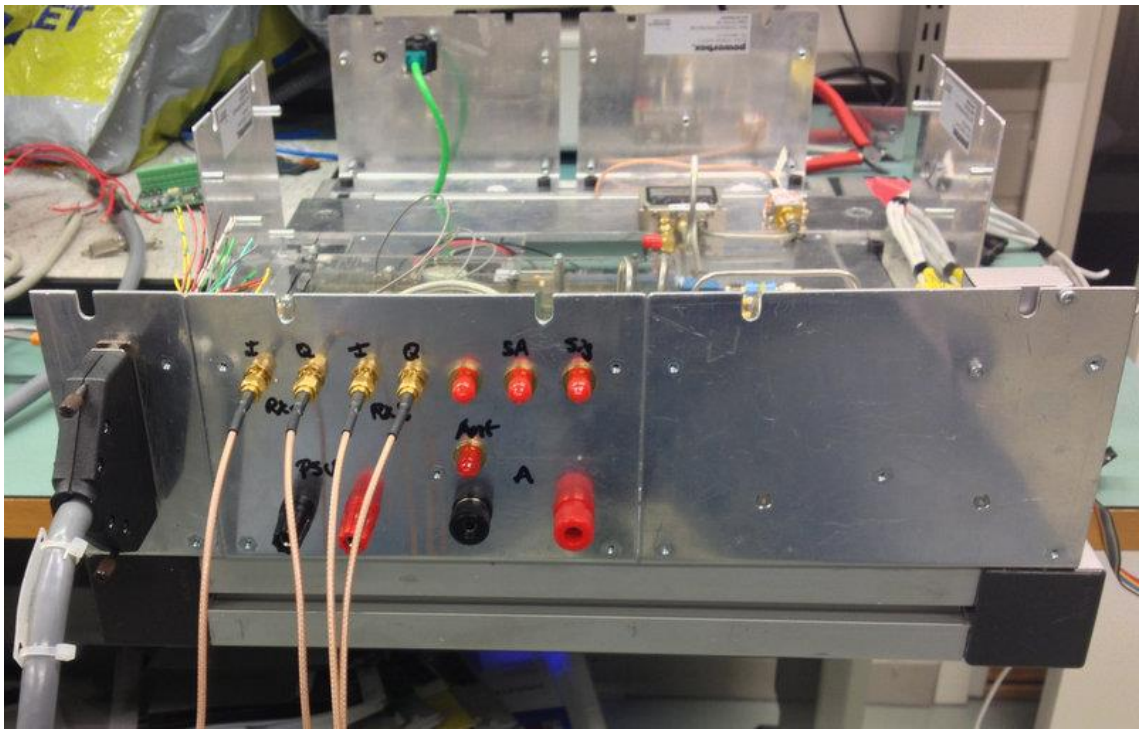

Figure 12. Test Fixture, Front View

The simple arrangement of the front panel connectors can be seen in Figure 12. The connector of the optional remote control for manual signal path routing and step attenuator control is installed in this early stage model, and can be seen to the left. The Test fixture was supplied with electrical power from three system power supplies. An additional supply for an embedded control module was established via PoE in the back of the fixture. The various sections of the transceiver card were all powered by their own external supplies in order to be able to establish a certain power-on sequence initiated by the fixture.

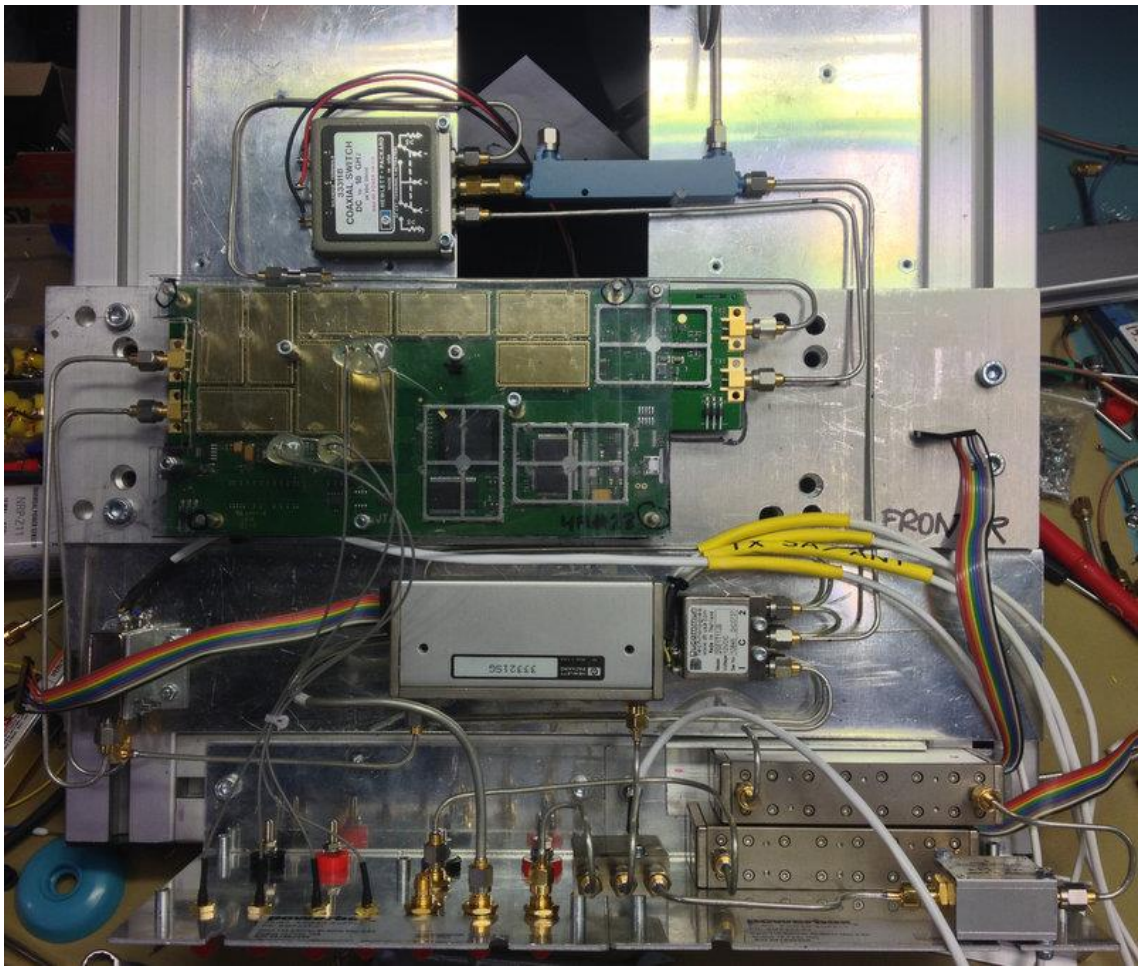

Figure 13. Test Fixture, Top View

Figure 13 shows a late stage of the fixture as seen from above. The front panel is in the bottom of the picture and the DUT is mounted near the centre. All signal connections were realised with semi-rigid solid copper coax to minimise the RF leakage.

4.5 Signal Routing

For the following paragraphs, it is necessary to be familiar with the system diagram illustrated by Figure 14. The test fixture consists of three major functional blocks:

- Transmitter related measurements (upper half of Figure 14),
- Receiver related measurements (lower right half of Figure 14),
- An antenna part that is shared by both the transmitter and receiver.

Additionally, there are a total of three connecting step attenuators used for isolation.

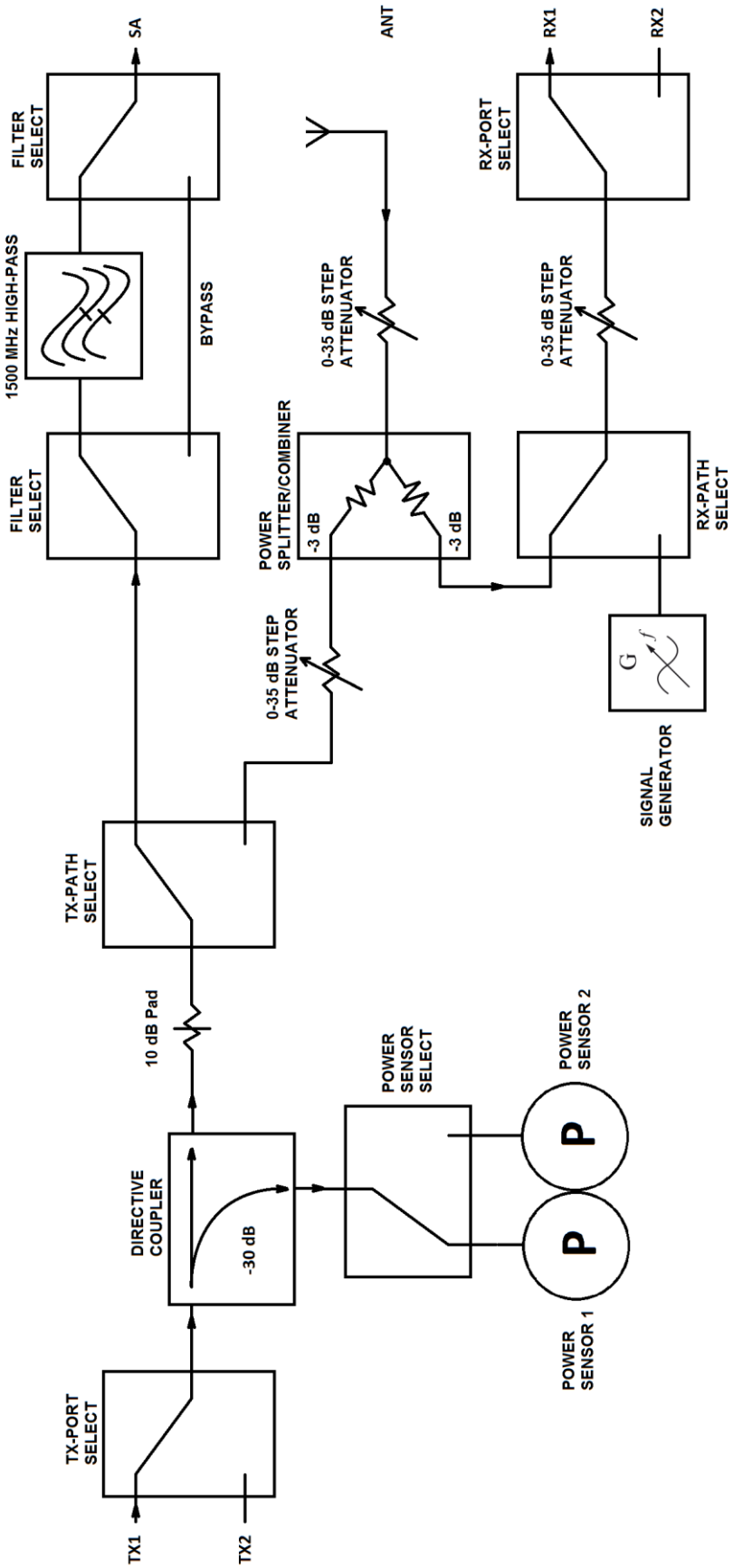

Figure 14. System Diagram of the Test Fixture RF-Signal Path

Starting with the two transmitter ports to the left, the very wide-band coaxial TX-PORT selection switch provides an easy way to choose between the two physical TX connectors of the DUT. As already seen early in section 3, most TX tests methods shall be repeated for all TX connectors, and since the DUT only uses one of them at any time a simple switch is sufficient. This reduces the number of performed mating cycles for cables and terminators and hence limits connector wear.

Then follows a directional coupler which couples the RF-power with -30 dB coupling to another very wide-band coaxial switch. This switch allows to choose between the two power sensors. This arrangement provides the means to conduct transmitter power measurements as required by the tests described in part 3.3.3.

Next, a 10 dB attenuator connects the signal from the directive coupler to the TX-PATH selection switch. When the upper path is selected the configuration will allow for frequency error, frequency stability, spectrum mask and spurious emissions measurements as described in sections 3.3.1 through 3.3.5. The FILTER SELECT switches, allow for an easy insertion of the high-pass filter mentioned in 3.3.5. Transmission time can either be measured with the commercial power sensor or with the TX-PATH selection switch set to the lower path, i.e. through the step attenuators, power divider and into the antenna. From here, an external oscilloscope probe can trigger from the transmission at the antenna.

The receiver block routes signals to the RX ports of the DUT from either of three possible signal paths. First, the RX-PATH selection switch can connect the signal generator to the RX ports for, for example, receiver sensitivity or spurious rejection tests as described in section 3.4.4. The other throw of the RX-PATH switch routes a signal received by an optional external antenna via step attenuators and a power divider to the RX ports, which in itself is not very useful as the tags operate via backscatter.

When however, the TX-PATH and the RX-PATH both are set to route to the antenna it is possible to have the transceiver interact with actual tags. It is imperative to be aware of the fact that the TX ports can carry powers in excess of 30 dBm, so that the receiver might be saturated. The 10 dB pad in the TX chain can only prevent catastrophic failure, therefore, the step attenuators are required to be set to a value that helps with the isolation between the TX and RX ports.

4.6 Power Measurements

The test fixture features two options for power measurement. The standard power sensor, sensor 1, is an expensive commercial R&S® NRP-Z11Three-Path Diode Power Sensor[9] with a measurement range from -67 dBm to +23 dBm. It was intended to be used for normal operation but due to a number of reasons it became necessary to find an alternative solution for the power measurement. As a result a second sensor, sensor 2, was implemented in the test fixture.

Sensor 2 is an inexpensive ZX47-40-S+ power detector from Mini-Circuits [14] with a measurement range from -40 dBm to +20 dBm and similar bandwidth as sensor 1. It converts RF-power at its input to a DC voltage at its output with a slope of -25 mV/dB.

The following requirements had to be addressed in order to make the power detector compatible with the test fixture:

- It needed a graphical user interface (GUI) for Labview
- It had to display instantaneous and peak power
- It needed a band switch to choose between 868 MHz and 915 MHz operation
- It had to provide power offset adjustment
- It needed a calibration procedure

All these requirements were met and are documented in appendices [C] and [D]. A proof-of-concept can further be found in appendix [E], in which 100 samples of RF-power from an EBS transmission through the test fixture are acquired with a sample rate of at least 30 readings per second. This shows that with the used equipment, Sensor 2 is able to meet the requirements for measuring the RF power as needed in the test method described in section 3. With an offset setting of +30.6815 dB, i.e. taking into account the loss from the TX connector all the way to the power sensor connector found in appendix [D], an input voltage u_{in} is converted to TX-power L_{TX} in dBm with (4-1):

Input voltage to TX-power conversion, 865 MHz

$$L_{TX}(dBm) = -2.9616 \cdot {u_{in}}^2 - 30.897 \cdot u_{in} + 66.214 \qquad (4\text{-}1)$$

[9] See Appendix B for measurement uncertainties of Sensor 1

With this, and the transmitter power and harmonic limits of Table 2, it is now possible to correctly measure the power output at the TX connector and compare it against the TX power limits in Table 4.

Table 4. TX Power Limits

Frequency [MHz]	ERP Test, peak Limit [dBm]	
	TX1	TX2
865	31.15	31.15
915	34.00	34.00

Table 4 assumes a circularly polarised antenna with a beamwidth of $\theta_{3\,dB} \leq 180°$, a maximum allowed ERP of 30.0 dBm for ETSI and 33.85 dBm FCC[10], cable loss of 1 dB for 1.5 m of RG58 and an antenna gain of 5 (868 MHz).

4.7 Harmonic Measurements

The path loss of the fixture from the TX connectors to the SA connector was evaluated with the commercial power Sensor 1 and an HP8648C signal generator, with and without the high-pass filter, for frequencies of the 1st, 2nd and 3rd harmonics for both the relevant ETSI and FCC frequency bands. The correction factors are summarised in Table 5:

Table 5. Path Loss, TX1/TX2 to SA Port

Frequency [MHz]	Bypass Loss [dB]		High-Pass Filter Loss [dB]	
	TX1	TX2	TX1	TX2
865	-11.60	-11.68	-52.40	-52.00
915	-11.64	-11.53	-51.48	-51.80
1730	-11.91	-12.21	-12.91	-13.07
1830	-11.86	-12.01	-12.74	-12.84
2595	-11.90	-12.25	-12.53	-12.74
2745	-11.70	-12.15	-12.15	-12.45

These correction factors must be taken into account when measuring harmonics.

[10] The FCC references assume that an antenna with 6 dBi is used. It was unclear whether this value is accounted for in Table 2.

5 Discussion/Review

The Test fixture was taken into use for production testing almost as soon as the RF-signal path was constructed and mounted on the fixture platform. Measurements conducted and corrected with the correction factors for path loss and harmonics appeared to be in agreement with past values and reference devices. Unfortunately this also slowed down the progress of the project, since the test fixture was in use most of the time.

During the course of the project a number of problems were discovered and dealt with. The fact that test equipment was scarce meant that instruments, in particular the commercial power meter, would have to be shared between different projects. To solve this issue, a low-cost power detector was evaluated and deemed sufficiently accurate to be used in the test fixture. A drawback of this sensor was that it required to be calibrated against the known commercial sensor in regular intervals. The advantage was the fact that it meant consistent, permanent use in the test fixture.

Another aspect was the fact that the test system would require a complete duplicate of the RF test fixture, and possibly also some key instruments for production scale-up. Scaling could become an issue if the amount of base stations to be tested would increase. However, this seems to be true for most RF-transceiver production testing.

Looking back; a bit of a disappointment was the fact that the controller of the DUT did not yet support a command interface which was needed to control the transmission of the DUT from the ATE. On the bright side, the amount of knowledge and experience gathered from the production testing and compliance testing was extensive. A lot of work lies in gathering and knowing the test specifications and regulations.

6 Conclusion

This thesis presented an overview of the test methods used in the testing of RFID base stations, specifically in the 868 MHz and 915 MHz ISM frequency bands. It explained EIRP, ERP and electric field strength and also provided the necessary tools to convert between them. Each test method was explained adequately and the thesis would provide a good base for anyone interested in transceiver testing.

A test fixture was developed which allowed to select between the aforementioned tests without the need of changing cables or connectors. This provided excellent improvements in terms of repeatability and reduced testing time for especially output power and harmonics measurements, which make up a large part of the device testing for MariSense Oy.

By using second-hand components, the total material cost for the test fixture amounted to less than 400 EUR [F]. This is a very competitive price given the high-quality signal path switching capability, the low-cost power sensor and the simple means by which the fixture was integrated into a semi-ATE system. Unfortunately, the lack of a proper interface to the controller unit of the DUT prevented the test system from being automated at the time the fixture was developed. This could be improved upon in a continuation of the project.

Future work could consist of adding automated calibration capability to the test system by providing for example additional signal path arrangements and logic that can evaluate and assess the path loss and power offset values. Another aspect that has been completely disregarded is temperature drift.

All in all it can be concluded that the project was a success and useful to MariSense Oy in that it proved to be a sturdy tool not only for R&D tasks, but for the device verification process of the Ella® Base Station, which it improved significantly.

References

[1] ECC, “REC 70-03,” 07 Feb 2014. [Online]. Available: http://www.erodocdb.dk/docs/doc98/official/pdf/rec7003e.pdf. [Accessed 24 April 2014].

[2] FCC, “47 CFR 15,” in *Title 47 Telecommunications, Radio frequency devices*, Office of the Fedreal Register, 2012.

[3] ITU, “Radio Regulations Articles,” 6 1 2012. [Online]. Available: http://life.itu.int/radioclub/rr/art05.htm#Reg. [Accessed 01 March 2014].

[4] M. Loy, R. Karingattil and L. Williams, “ISM-Band and Short Range Device Regulatory Compliance,” May 2005. [Online]. Available: http://www.ti.com/lit/an/swra048/swra048.pdf. [Accessed 2 Feb 2014].

[5] ETSI, “EN 302 208-1,” Nov 2011. [Online]. Available: http://www.etsi.org/deliver/etsi_en/302200_302299/30220801/01.04.01_60/en_30220801v010401p.pdf. [Accessed 1 May 2014].

[6] FCC, “47 CFR 15.247,” in *Title 47 Telecommunications, Operation within the bands 902-928 MHz, 2400-2483.5 MHz, and 5725-5850 MHz.*, Office of the Fedreal Register, 2012.

[7] ETSI, “ETSI ETR 028,” April 1992. [Online]. Available: http://www.etsi.org/deliver/etsi_etr/001_099/028/01_60/etr_028e01p.pdf. [Accessed 1 May 2014].

[8] S. Winder and J. Carr, Radio and RF Engineering Pocket Book, London: Newnes, 2002.

[9] F. H. Sanders, “Institute for Telecommunication Sciences,” U.S. Dept. of Commerce, June 2010. [Online]. Available: http://www.its.bldrdoc.gov/publications/2507.aspx. [Accessed 1 May 2014].

[10] ECC, “REC 70-03 Annex 11 b2,” 07 Feb 2014. [Online]. Available: http://www.erodocdb.dk/docs/doc98/official/pdf/rec7003e.pdf. [Accessed 24 April 2014].

[11] EC, “Harmonised standards under Directive 1999/5/EC,” [Online]. Available: http://ec.europa.eu/enterprise/sectors/rtte/documents/standards/index_en.htm. [Accessed 1 May 2014].

[12] IEEE, “ANSI C63.4-2009,” 15 September 2009. [Online]. Available: http://ieeexplore.ieee.org/servlet/opac?punumber=5246987. [Accessed 8 May 2014].

[13] Texas Instruments, “Understanding and Enhancing Sensitivity in Receivers for Wireless Applications,” 1999. [Online]. Available: http://www.ti.com/lit/an/swra030/swra030.pdf. [Accessed 9 May 2014].

[14] Mini-Circuits, “ZX47-40+ Coaxial Power Detector,” [Online]. Available: http://217.34.103.131/pdfs/ZX47-40+.pdf. [Accessed 5 May 2014].

[15] D. M. Pozar, Microwave Engineering, Amherst, Massachusetts: Wiley, 2012.

[16] Rhode&Schwarz, “RF Level Measurement Uncertainties with the Measureing Receiver R&S FSMR,” March 2006. [Online]. Available: http://cdn.rohde-schwarz.com/dl_downloads/dl_application/application_notes/1ma92/1MA92_0e_RF_level_meas_uncertainties.pdf. [Accessed 5 May 2014].

[17] ETSI, “ETSI EN 300 220-2,” May 2012. [Online]. Available: http://www.etsi.org/deliver/etsi_en/300200_300299/30022002/02.04.01_60/en_30022002v020401p.pdf. [Accessed 1 May 2014].

[18] ETSI, “EN 300 440-1,” August 2010. [Online]. Available: http://www.etsi.org/deliver/etsi_en/300400_300499/300440/01.02.01_20/en_300440v010201c.pdf. [Accessed 1 May 2014].

[19] Agilent Technologies, “User's Guide - 8590 E-Series and L-Series Spectrum Analyzers,” July 1998. [Online]. Available: http://cp.literature.agilent.com/litweb/pdf/08590-90301.pdf. [Accessed 4 May 2014].

[20] EC, “Guide to the R&TTE Directive 1999/5/EC,” April 2009. [Online]. Available: http://ec.europa.eu/enterprise/sectors/rtte/files/guide2009-04-20_en.pdf. [Accessed 12 May 2014].

Appendix A – From Electric Field Strength to EIRP

For an antenna matched to a load, the received power in in the load p_{load} is related to the free space power density p_{den} by the effective antenna aperture a_e:

$$p_{load} = p_{den} \cdot a_e$$

If further p_{den} is in a free-space impedance of 377 Ω, then the following relation applies:

$$p_{den} = \frac{V_{space}^2}{377\Omega} = \frac{E^2}{377\Omega}$$

Where E is the free-space field strength of unit $\frac{V}{m}$.

The effective antenna aperture $a_e = \frac{\lambda^2 g}{4\pi}$ of an antenna is the effective aperture of a theoretical isotropic antenna multiplied by the actual antenna gain of the receiving antenna g_r over isotropic:

$$a_e = \frac{\lambda^2}{4\pi} g_r$$

The received power in in the load p_{load} can therefore be expressed as:

$$p_{load} = \frac{E^2}{377\Omega} \cdot \frac{\lambda^2}{4\pi} g_r$$

Further, the effective isotropic radiated power $eirp$ with transmit power p_t and transmit antenna gain relative to isotropic g_t is:

$$eirp = p_t \cdot g_t$$

Additionally, with Friis' transmission equation for the ratio of received to transmitted power $\frac{p_r}{p_t}$ available for two antennas with gain g_r and g_t with respect to an isotropic radiator:

$$\frac{p_r}{p_t} = g_r \cdot g_t \cdot \left(\frac{\lambda}{4\pi r}\right)^2 \Leftrightarrow p_r = p_t \cdot g_t \cdot g_r \cdot \left(\frac{\lambda}{4\pi r}\right)^2$$

The following equality equation is solved for $EIRP$:

$$p_{load} = p_r$$
$$\frac{E^2}{377\Omega} \cdot \frac{\lambda^2}{4\pi} g_r = p_t \cdot g_t \cdot g_r \cdot \left(\frac{\lambda}{4\pi r}\right)^2$$
$$\frac{E^2}{377\Omega} \cdot \frac{\lambda^2}{4\pi} g_r = p_t \cdot g_t \cdot g_r \cdot \frac{\lambda^2}{4^2\pi^2 r^2}$$
$$\frac{E^2 4^2 \pi^2 r^2 \lambda^2}{377\Omega \cdot 4\pi \cdot \lambda^2} \cdot g_r = p_t \cdot g_t \cdot g_r$$
$$p_t \cdot g_t = \frac{E^2 \cdot 4\pi \cdot r^2}{377\Omega}$$
$$eirp = \frac{E^2 \cdot 4\pi \cdot r^2}{377\Omega}$$
$$\frac{eirp}{1mW} = \frac{4\pi \cdot E^2 \cdot r^2}{1mW \cdot 377\Omega}$$
$$10 \cdot \log\left(\frac{eirp}{1mW}\right) dBm = 10 \cdot \log\left(\frac{4\pi \cdot E^2 \cdot r^2}{1mW \cdot 377\Omega}\right) dBm$$
$$EIRP = 10 \cdot \log\left(\frac{4\pi \cdot E^2 \cdot r^2}{0.377\ [V^2]}\right) dBm$$
$$EIRP = 10 \cdot \log\left(\frac{4\pi \cdot E^2 \cdot r^2}{0.377\ [V^2]}\right) dBm$$
$$= 10 \cdot \log\left(\frac{E^2 \cdot r^2}{0.030\ [V^2]}\right) dBm$$

Where:

$EIRP$: The Effective Isotropic Power in *dBm*,

E : The electrical field strength in $\frac{V}{m}$

r : The distance from the transmitting antenna in *m*, and

V : is the unit of measurement (*Volt*).

Reference: [9, pp. 2-3, 11] [15, p. 674]

Appendix B – Power Sensor 1 Measurement Uncertainties

Absolute uncertainty (+20…+25 C): 0.047 to 0.083
Relative uncertainty (+20…+25 C): 0.022 to 0.066
VSWR 10 MHz to 2.4 GHz: < 1.13, VSWR 2.4 GHz to 8.0 GHz: < 1.2

Sources of error: (Absolute power)
The measurement uncertainty of the sensor is the main source
Sensor specs and mismatch (VSWR) between source and sensor
Mismatch of the source (VSWR) and cable loss
Linearity error
Range-to-range error (three diodes)
Temperature drift
Zero-offset and drift
Display noise
Statistical measurement uncertainty (type A) SNR at low powers

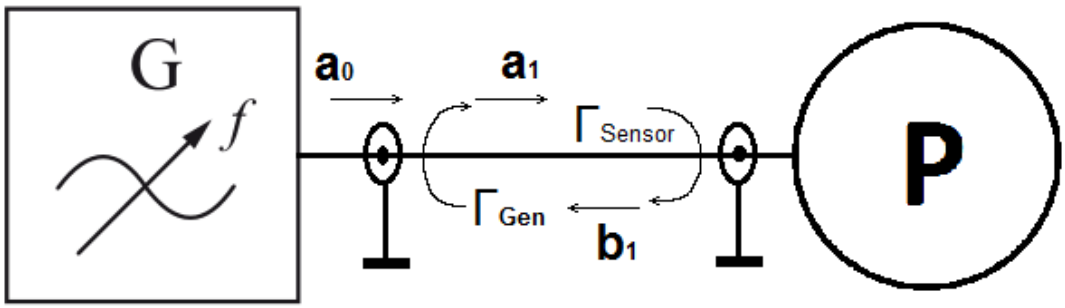

$$\frac{a_1}{a_0} = \frac{1}{1 - \Gamma_{Sensor} \cdot \Gamma_{Gen}}$$

Where:
a_0: The forward wave (matched case)
a_1: The resulting forward wave ($a_1 = a_0 + b_1 \cdot \Gamma_{Sensor}$)
b_1: The resulting return wave caused by a_1 reflected at Γ_{Sensor} ($b_1 = a_1 \cdot \Gamma_{Sensor}$)
Γ_{Gen}: The reflection coefficient of the generator output
Γ_{Sensor}: The reflection coefficient of the power sensor input
Reference: [16, pp. 12, 15]

Appendix C – Power Sensor 2, LabVIEW Code

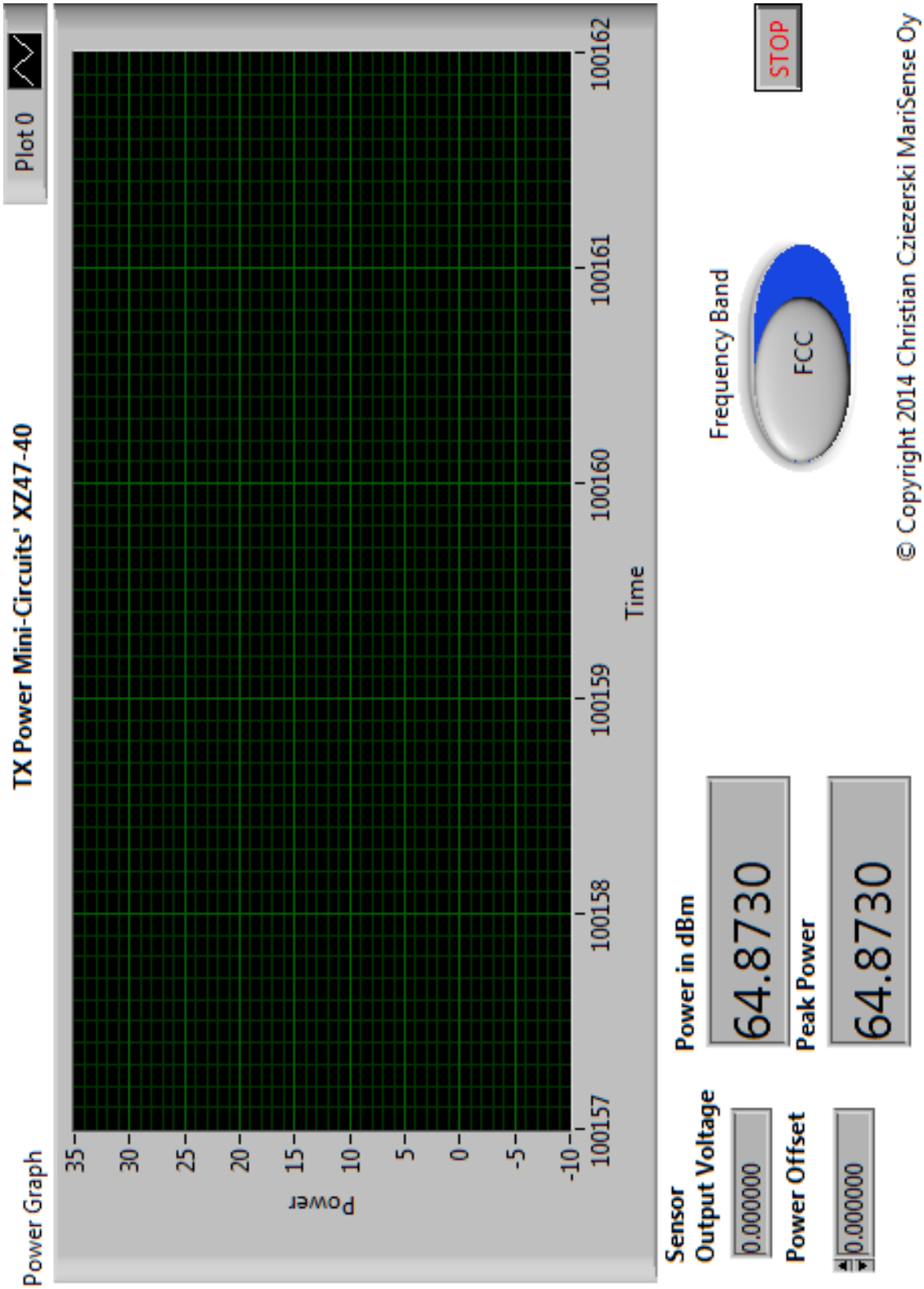

Figure C-1. Power Sensor 2, LabVIEW GUI

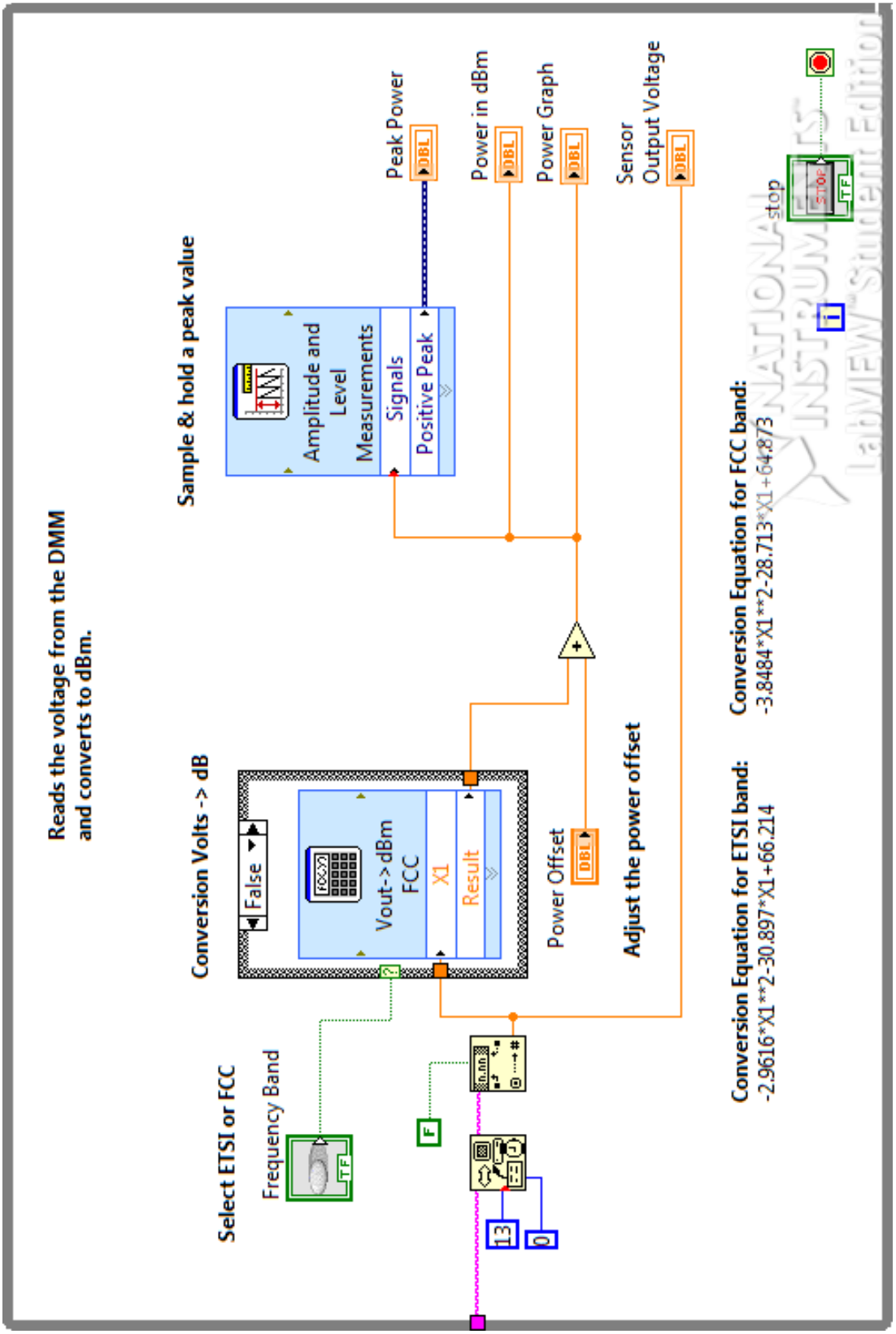

Figure C-2. Power Sensor 2, Main LabVIEW Code

Appendix D – ZX47-40S+ Power Sensor, Matlab Power Detector Calibration

```
% This MATLAB script steps the output power of an HP8648B
% at 10MHz from -50 dBm to +12 dBm in steps of 0.1 dBm.
% Copyright 2013 Christian Cziezerski, created for MariSense Oy Finland

% clear variables
clear dec;
clear vec;
clear amplitude;
clear inputpower;

% set variables
% Amplitude setting
amplitude_min = -50;
amplitude_max = 0;
amplitude = amplitude_min;

% the number of samples to capture (100 per 10 dB) -50 = 641
readings = 501;

% try-catch
% if anything goes wrong in this loop, the instrument session will be
% closed in an orderly manner and any error that occured is thrown back.
try
    % ***** DMM setup *****
    % create an instrument object for the DMM and open a session
    % the GPIB instrument address is 10
    HP3478A = visa('agilent', 'GPIB0::10::INSTR');
    fopen(HP3478A);

    % setup the DMM to measure:
    % Z0 - auto zero off, to speed up the measurement
    % N4 - 4_1/2 digits display, 1 PLC integration
    % F1 - Measurement Mode DCV
    % R0 - volt range 3 V,
    % T1 - Internal trigger
    % D3 - Display a custom text on the display and disable update
    % this ensures approximately 30 readings/s, if a higher readings/s is
    % required, the 3_1/2 digit mode (N3) provides ca 85 readings/s
    fprintf(HP3478A, '%s\r', 'Z0N4F1R0T1D3READING...');

    % ***** SigGen setup *****
    % create an instrument object for the SigGen and open a session.
    % the GPIB instrument address is 19
    HP8648B = visa('agilent', 'GPIB0::19::INSTR');
    fopen(HP8648B);

    % setup the SigGen to initial condition.
    %
    % --- Amplitude ---
    % "OUTP:STAT OFF"   - Output OFF
    % "POW:AMPL -50 DBM"
    % --- Frequency ---
    % "FREQ:CW 10 MHz"  - set f = 10.00000 MHz
    % --- Modulation ---
    % AM, FM, PhiM, PM off per default
    % modulation OFF
    %
    fprintf(HP8648B, ['OUTP:STAT ON;:POW:AMPL ' num2str(amplitude) ' DBM;:FREQ:CW 10
MHz']);

    % Wait for RF output power to settle
    pause on;
    pause(2);

    % ***** Main program part *****
    % ***** Sig gen power sweep *****
    % Gather data from the DMM
    for i = 1:readings
        % Send power setting to instrument
        fprintf(HP8648B, ['POW:AMPL ' num2str(amplitude)]);
```

```
        pause(0.1);
        % measure the power sensor voltage
        vec(i) = str2num(fscanf(HP3478A));
        inputpower(i) = amplitude;
        pause(0.1);
        % display the measured voltage value
        disp(['Power set to ' num2str(amplitude) '. VDC reading ' num2str(i) ' = '
num2str(vec(i)) ' V.']);
        amplitude = amplitude + 0.1;
    end

    % Re-enable autozeroing and the display
    fprintf(HP3478A, 'Z1D1');
    %disable SigGen output
    fprintf(HP8648B, 'OUTP:STAT OFF');

    % close the connection to the instrument and remove the VISA object
    fclose(HP8648B);
    delete(HP8648B);
    clear HP8648B;

    fclose(HP3478A);
    delete(HP3478A);
    clear HP3478A;

    disp('done');

catch err

    pause off;
    % Re-enable autozeroing and the display
    fprintf(HP3478A, 'Z1D1');
    %disable SigGen output
    fprintf(HP8648B, 'OUTP:STAT OFF');

    % close connection and instruments and remove VISA object
    fclose(HP8648B);
    delete(HP8648B);
    clear HP8648B;

    fclose(HP3478A);
    delete(HP3478A);
    clear HP3478A;

    % return any error in an orderly manner
    rethrow(err);
end

% convert the voltage vector to an ETSI power in dBm
dec = (-2.9616*vec.^2-30.897*vec+66.214);

%implement a switch between ETSI / FCC

% % Plot the voltage
% figure
% plot(vec)
% title('Power measurement with ZX47')
% xlabel('Reading Number')
% ylabel('dBm')
% grid on

% Plot the power
figure
plot(inputpower,vec)
title('Power measurement with ZX47')
ylabel('Sensor Voltage [V]')
xlabel('Sensor Power [dBm]')
grid on
```

The recorded values are used to calculate a 2nd order approximation of the output voltage graph vs. input frequency for both frequency bands as seen in figures D1 and D2:

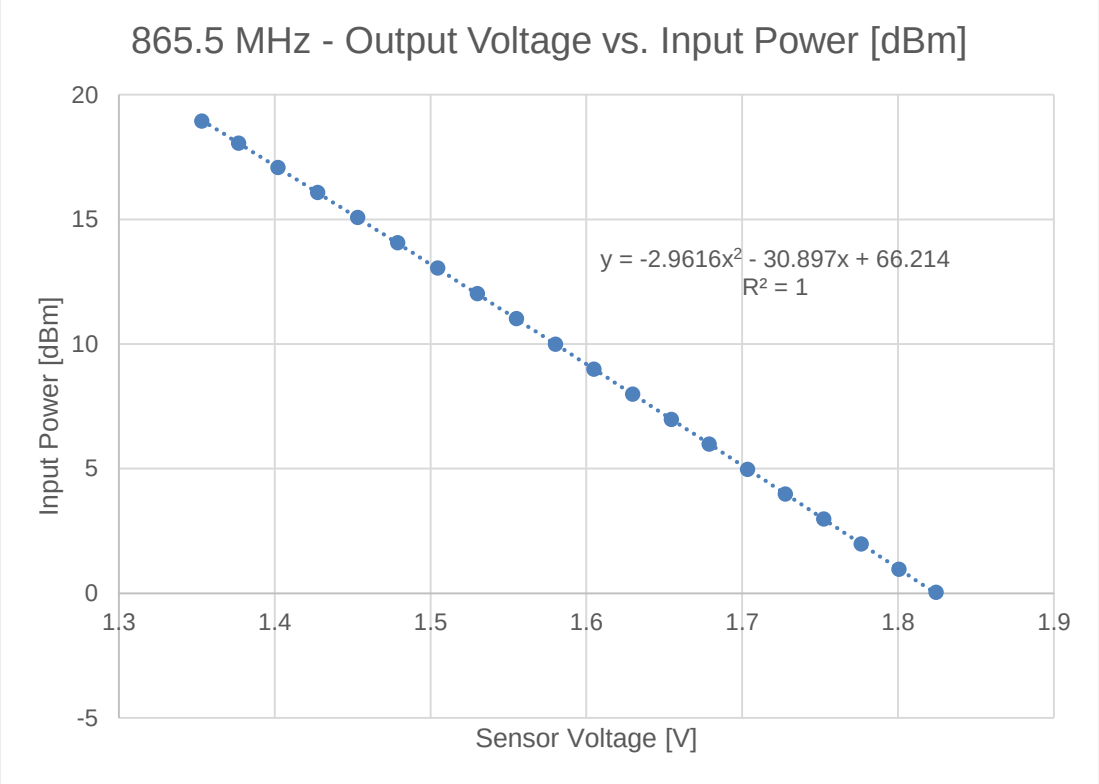

Figure D-1. Power Sensor 2, Second Order Correction Factors for 865.5 MHz

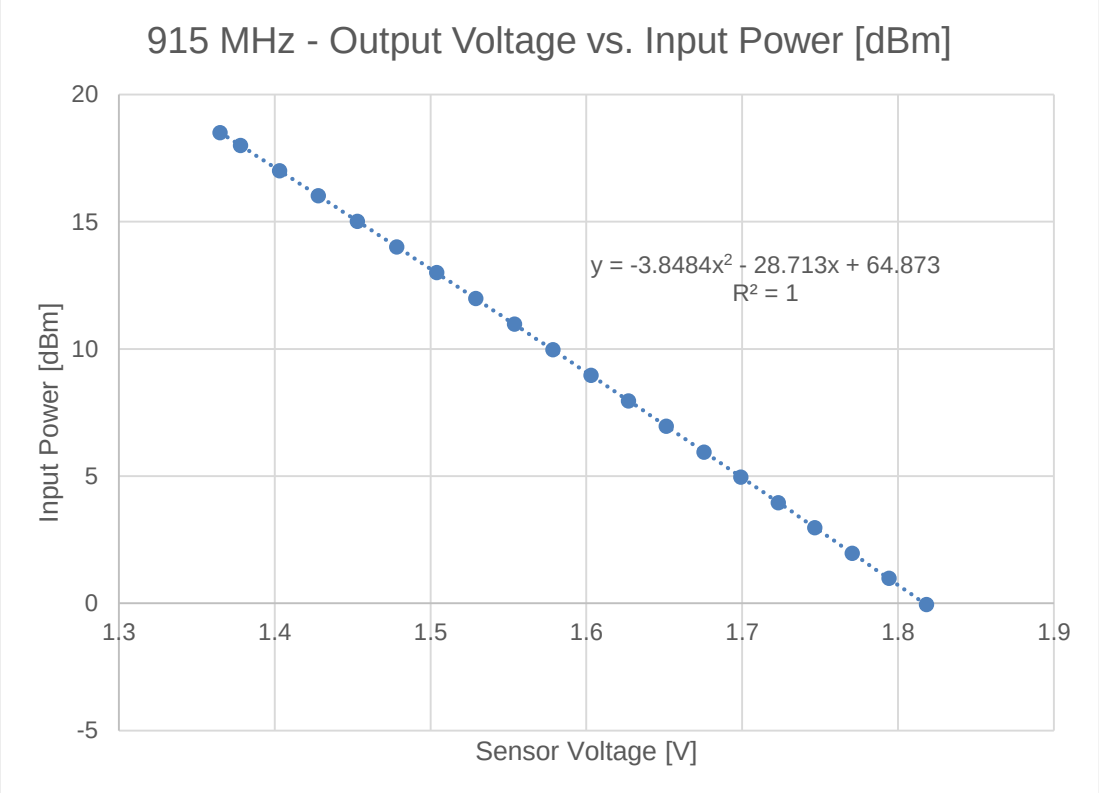

Figure D-2. Power Sensor 2, Second Order Correction Factors for 915 MHz

Table D-1. Power Sensor 2, In-House Calibration Values for FCC 915 MHz

dBm In	Volt Out	Direct	Offset
-0.04	1.8182	30.64	30.68
0.98	1.7942	31.65	30.67
1.97	1.7706	32.65	30.68
2.97	1.7467	33.65	30.68
3.96	1.7231	34.64	30.68
4.96	1.6992	35.64	30.68
5.94	1.6756	36.63	30.69
6.96	1.6513	37.64	30.68
7.96	1.6271	38.64	30.68
8.96	1.6030	39.64	30.68
9.97	1.5785	40.65	30.68
10.98	1.5539	41.66	30.68
11.99	1.5290	42.67	30.68
13.00	1.5040	43.68	30.68
14.01	1.4784	44.70	30.69
15.02	1.4531	45.71	30.69
16.02	1.4280	46.70	30.68
17.01	1.4031	47.69	30.68
18.00	1.3780	48.68	30.68
18.50	1.3650	49.19	30.69

The power levels in the “dB In” column in Table D-1 were generated with an HP8648B signal generator at a constant frequency of 915 MHz. The absolute power level was verified with Sensor 1, meanwhile the Sensor 2 output voltage was measured with an HP3478A multimeter and recorded in the “Volt Out” column in Table D-1. From this, the 2nd order approximation is calculated and used as correction factor in the LabVIEW main code for 915 MHz.

The values in the “Direct” column are the uncorrected values, i.e. without taking the coupling factor of the directive coupler or RF-relay insertion loss into account. The “offset” column is the difference between the uncorrected “Direct” values and the absolute “dB In” values. This indicates, that the attenuation from the connector of the TX input switch to the input of power Sensor 2 is an average of -30.6815 dB. This is the value that must be entered in the power sensor 2 LabVIEW GUI.

Table D-2. Power Sensor 2, In-House Calibration Values ETSI 865.5 MHz

dBm In	Volt Out
0.03	1.8244
0.96	1.8007
1.98	1.7763
2.98	1.7523
3.98	1.7277
4.97	1.7035
5.98	1.6789
6.97	1.6546
7.98	1.6297
8.99	1.6049
9.99	1.5802
11.01	1.5551
12.02	1.5300
13.04	1.5046
14.06	1.4789
15.08	1.4532
16.08	1.4276
17.08	1.4021
18.05	1.3768
18.94	1.3500

Similar to the measurement conducted for the 915 MHz calibration, the absolute power values in the “dB In” column were measured with Sensor 1 at 865.5 MHz and the power detector output voltage measured with a multimeter and recorded in the “Volt Out” column. From this, the 2nd order approximation is calculated and used as correction factor in the LabVIEW main code for 868.5 MHz.

Appendix E – ZX47-40S+ Power Sensor, Matlab DAQ Script

```
% This MATLAB script collects 100 samples from an HP3478A DMM and converts
% the reading to a power in dBm. The sensor input range is ca 0.2 to 2.2 Volt
% Copyright 2013 Christian Cziezerski, created for MariSense Oy Finland

% clear variables
clear dec;
clear vec;

% try-catch
% if anything goes wrong in this loop, the instrument session will be
% closed in an orderly manner and any error that occured is thrown back.
try
    % create an instrument object for the DMM and open a session
    % the GPIB instrument address is 10
    HP3478A = visa('agilent', 'GPIB0::10::INSTR');
    fopen(HP3478A);

    %get(HP3478A, 'Status'); % future test for active session

    % setup the DMM to measure:
    % Z0 - auto zero off, to speed up the measurement
    % N4 - 4_1/2 digits display, 1 PLC integration
    % F1 - Measurement Mode DCV
    % R0 - volt range 3 V,
    % T1 - Internal trigger
    % D3 - Display a custom text on the display and disable update
    % this ensures approximately 30 readings/s, if a higher readings/s is
    % required, the 3_1/2 digit mode (N3) provides ca 85 readings/s
    fprintf(HP3478A, '%s\r', 'Z0N4F1R0T1D3READING...');

    % the number of samples to capture
    readings = 100;

    % Gather data from the DMM
    for i = 1:readings
        vec(i) = str2num(fscanf(HP3478A));
        disp(['VDC reading ' num2str(i) ' = ' num2str(vec(i)) ' V.']);
    end

    % Re-enable autozeroing and the display
    fprintf(HP3478A, 'Z1D1');

    % close the connection to the instrument and remove the VISA object
    fclose(HP3478A);
    delete(HP3478A);
    clear HP3478A;

    disp('done');

catch err

    % Re-enable autozeroing and the display
    fprintf(HP3478A, 'Z1D1');

    % close connection and instrument and remove VISA object
    fclose(HP3478A);
    delete(HP3478A);
    clear HP3478A;

    % return any error in an orderly manner
    rethrow(err);
end

% try to get a better default scale and axis ticks
% set(gca,'YTickLabel',num2str(get(gca,'YTick').'))
% x=[4000, 8000, 10000, 12000]; % define the x values where you want to have a tick
% set(gca,'XTick',x);  % Apply the ticks to the current axes
% set(gca,'YTickLabel', arrayfun(@(v) sprintf('%d',v), x, 'UniformOutput', false) ); %
Define the tick labels based on the user-defined format
```

```
% convert the voltage vector to an ETSI power in dBm
dec = (-2.9616*vec.^2-30.897*vec+66.214);

%implement a swtich between ETSI / FCC

% Plot the power
figure
plot(dec)
title('Power measurement with ZX47')
xlabel('Reading Number')
ylabel('dBm')
grid on
%plot(tline(1,1:readings),'DisplayName','tline(1,1:readings)','YData-
Source','tline(1,1:readings)');figure(gcf);
```

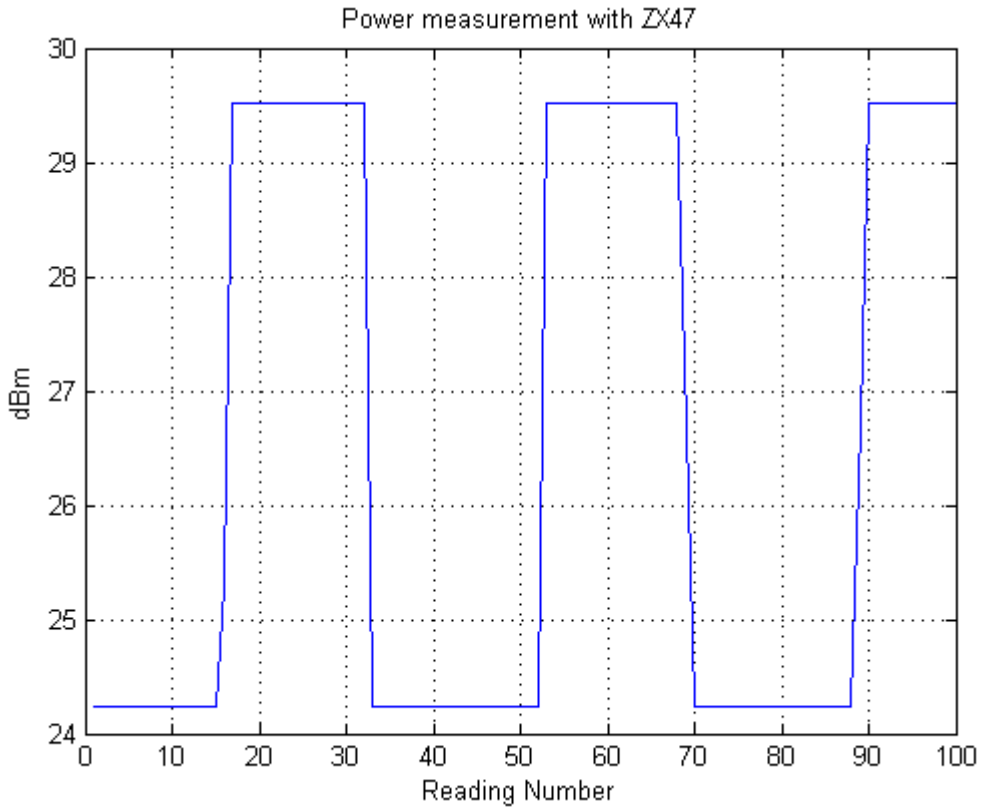

Figure C-1. Sample ZX47-40 Power Measurement Output

Figure C-1 illustrates a proof-of-concept of an EBS TX RF-signal converted from sensor voltage output to dBm scale for the 868 MHz band. The sensor voltage is converted into power with the formula found in appendix [D]:

Power = (-2.9616*uin.^2-30.897*uin+66.214)

Appendix F – Parts List

Nr.	#	Item	Piece	Total
1	1x	Directive Coupler, S.M. Electronics MC3202-20	-	-
2	3x	Step Attenuator, HP 33321SG DC to 4 GHz, 0-35 dB	45.33	135.99
3	1x	Power Splitter/Combiner, Mini-Circuits ZFSC-2-2-S 10-1000 MHz	-	-
4	2x	Coaxial Switch, HP 33311B DC to 18 GHz	28.525	57.05
5	2x	Coaxial Relay, Ducommun 2SE1T11JB, DC to 26.5 GHz	21.945	43.89
6	2x	Coaxial Relay, Ducommun 2SE1T11JB, DC to 26.5 GHz	7.02	14.04
7	2x	Coaxial Relay, Ducommun 2SE1T11JB, DC to 26.5 GHz	13.81	27.62
8	10x	push button switch, 1A ,125VAC, black	1.339	13.39
9	5x	Panel mount adapter, SMA-SMA, bulkhead O-ring	2.722	13.61
10	9x	miniature toggle switch, 1-pole (on)/off/(on)	-	-
11	13x	Semi-rigid coax 0.085 + 2x SMA connector	2.48	32.24
12	2x	Semi-rigid coax 0.141 + 2x SMA connector	-	-
13	1x	MHz Power Detector, Mini-Circuits ZX47-40-S+, -40 to +20 dBm, 10-8000 MHz	37.18	37.18
		Total		375.01

Appendix G – Photographs

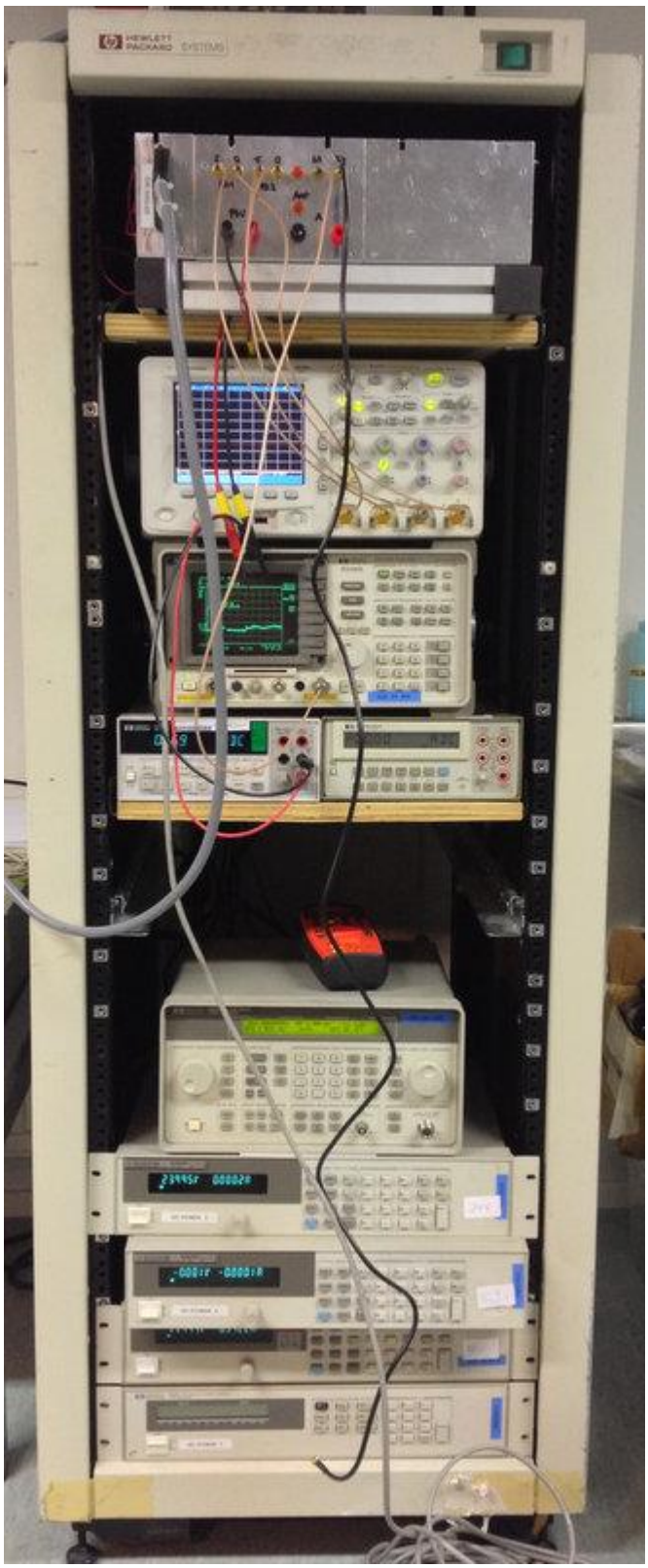

Figure G-1. Complete Test Rack with Test Fixture

Figure G-2. Test Rack Remote Control

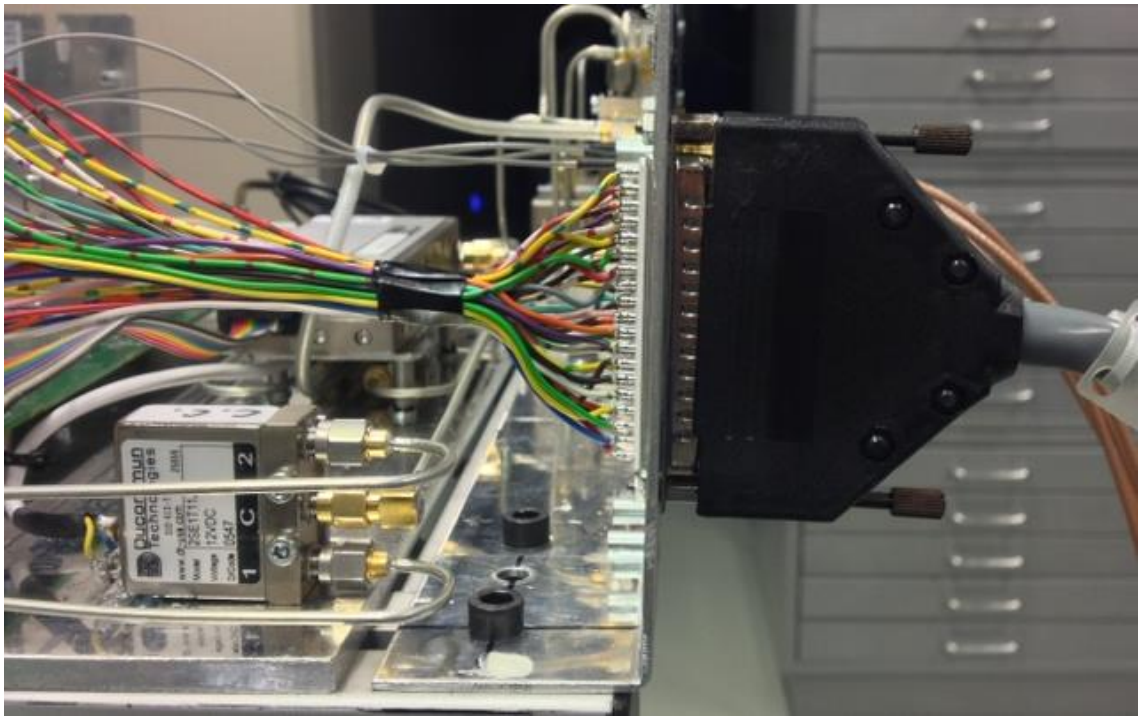

Figure G-3. Test Rack ATE Connector